

DISC PADS

CALIPER ASSEMBLY

WHEEL BEARING

WHEEL STUDS

THE EFFECT OF GEOPOLYMER MATERIALS ADDITIVES IN BRAKE FRICTION MATERIALS

Gökçen AKGÜN



DUJAR

**THE EFFECT OF
GEOPOLYMER MATERIALS
ADDITIVES IN BRAKE FRICTION
MATERIALS**

Gökçen AKGÜN



The Effect of Geopolymer Materials Additives In Brake Friction Materials
Gökçen AKGÜN

Editor in chief: Berkan Balpetek

Cover and Page Design: Duvar Design

Printing : February -2024

Publisher Certificate No: 49837

ISBN: 978-625-6643-68-0

© Duvar Publishing

853 Sokak No:13 P.10 Kemeraltı-Konak/Izmir/ Turkey

Phone: 0 232 484 88 68

www.duvaryayinlari.com

duvarkitavevi@gmail.com

TABLE OF CONTENTS

Preface	4
1.Introduction	5
2.Selection and Production Methods of Brake Friction Materials	7
2.1. Selection and Classification of Brake Friction Materials	7
2.2. Production Methods of Brake Friction Materials	10
3. Geopolymers and Production of Geopolymer Additive Brake Friction Materials	13
3.1. Geopolymers.....	13
3.2. The Practical Applications of Geopolymers.....	20
3.3. Mechanical Properties of Geopolymer Materials	22
3.4. Production of Geopolymer Additive Brake Friction Materials	32
References	34

Preface

As with all products worldwide, there is a high demand for components in the automotive sector. In automotive technology, braking force and one of its essential components, the brake pad, are indispensable safety mechanisms for reducing or stopping the dynamic speeds of vehicles. Brake pads form a composite structure with multiple materials as components. The braking system is complemented by brake discs, the counter element to the brake pads. The halting of the moving system is achieved through the opposing forces generated by the friction between the two surfaces in contact. The presence of particles detached from brake pads during friction has become increasingly important over time. To reduce the chemicals polluting the atmosphere of our planet, the materials in brake pads need to be selected to be more environmentally friendly and nature-friendly. Therefore, using geopolimer material, an inorganic matrix, instead of phenolic resin as the matrix in brake pads can be much more effective. Not only is it environmentally friendly, but it also exhibits behavior that is both frugal in the face of material wear in brake pads and prevents excessive heating against the brake disc. Additionally, utilizing specific components with hydraulic activity to enable the complete hardening of friction material in an alkaline environment as an "alkali-activated" inorganic binder can positively contribute to both strength and friction properties in the development of new products. Thus, it is observed that geopolimer-derived materials are particularly used as a binding material in brake pads. The study provides insights into brake pads, materials, geopolimer materials, and their use as a next-generation binder in brake pads.

Throughout the study, I extend my thanks to my beloved wife Şemsi AKGÜN, who periodically came to check the progress of the book, my dear daughter Betül Asya, who occasionally visited me, and my valued friend Assistant Prof. Fethi ŞERMET, who remarked that this study should not be prolonged.

1.Introduction

Brake pads and discs constitute a significant wear pair in automotive brake systems. This duo is also commonly used in mechanical and industrial sectors outside of automotive systems. Their primary function is to safely and quickly stop a rotating system within safety limits [1]. Hence, developing new-generation brake pad materials has been a focus of researchers in the last quarter-century, continuously gaining prominence in studies [2, 3]. In fact, leading European countries (France and Germany) are preparing significant legislation to reduce emissions associated with this wear pair in brake systems [4]. The friction composite materials that make up brake pads fundamentally consist of four main material groups: binders, fillers, reinforcers, and friction modifiers [5, 6]. Binder materials, which are crucial in pad friction materials, are generally known to be made up of phenolic and rubber-based polymer composites [7]. Recently, there has been significant research and evaluation into alternative materials to replace phenolic resin, which holds a major place among binder materials [8-11].

The effect of the binder in brake pad friction materials plays a significant role in the friction characteristics of the entire structure. In a study on this subject, it was mentioned that the addition of geopolymers in brake pad friction materials reduces the amount of phenolic resin, which releases volatile organic compounds when exposed to temperatures above 300°C [2, 9]. Another study emphasized that geopolymers have better thermal properties than organic resins, which typically decompose by oxidation starting from 400°C [12]. The use of geopolymer-enhanced brake pads, a potential natural resource candidate in the production of next-generation brake pads, is presented as having advantages in terms of both reducing harmful dust particles released into the environment, thus benefiting healthy respiration, and being less costly compared to standard conventional brake pads [1]. It has been stated that geopolymer materials are used not only as binders but also as fillers in brake pad friction composite materials [1, 9]. The preference for using geopolymers, inorganic polymers, in brake pads is due to their excellent impact in maintaining mechanical properties as well as their thermal and corrosion resistance [13]. Such geopolymers containing organic fibers are known to create an excellent protective shield against fire [14-17]. They are also known as materials that harden quickly and have superior durability performance for rapid repair [18]. In the mechanical strength of geopolymer materials, alkali cations present in their structure play an effective role, balancing the negative charges associated with tetrahedral aluminate units that combine with silicate units to form a three-dimensional structure. It is stated that these balancing cations are alkali metal ions, and due to cost reasons, Na⁺ ions are more commonly used. However, it has been underlined that the use of K⁺ ions is

possible to increase the strength of the product. This leads to the formation of silicate oligomers preferred by the aluminate integrity, and improved hardening and compressive strength compared to geopolymers synthesized using NaOH [19, 20]. Furthermore, geopolymer matrices, which have a brittle structure, are increasingly gaining mechanical strength with fiber additions in the composites created [21, 22]. In the fire resistance of geopolymers, it has been mentioned that those activated with potassium-containing alkali activators have better fire resistance than those activated with sodium [23]. The fire resistance of geopolymers lies in the more stable properties of the compounds formed by the Si element in their structure with oxygen and other elements. It is stated that geopolymer foam materials show good strength resistance up to 400°C and continue to increase in strength beyond 800°C with increased heat. A similar crystallization-strengthening effect is encountered in other studies [24, 25]. Similar to metakaolin-based geopolymers, there are several factors affecting the thermal stability of fly ash-based geopolymers, such as the Si/Al ratio, type of alkali, and structure of the fly ash. According to the studies, the fire resistance depends on the source of the fly ash. For samples tested by heating at 1000°C, it was stated that both Eraring and Tarong fly ashes contain higher mullite content than Collie fly ash [25, 26]. As can be understood from these explanations, geopolymers derived from fly ashes, in particular, exhibit high temperature resistance.

The inclusion of various industrial wastes in the production of geopolymer materials, such as fly ash, steel furnace slag, and brake pad waste, enhances their appeal in terms of recycling. In this context, Bai et al. have created a metakaolin (MK) based geopolymer material using these types of industrial wastes [27]. Additionally, recent concerns in the automotive industry regarding the health hazards of copper in brake friction materials, particularly to aquatic life, have led to efforts to replace copper with suitable alternative materials [28-30]. In this scope, studies have shown that geopolymers are among the alternative materials that can replace copper [9].

The existence of such studies will contribute significantly to a healthy, livable atmosphere on Earth, while also reducing material and energy consumption and benefiting the global economy.

2. Selection and Production Methods of Brake Friction Materials

2.1. Selection and Classification of Brake Friction Materials

The components of brake friction materials produced for the brake pads of vehicles in the automotive sector for new generation or for the development of existing ones are formed by combining 10 or more different raw materials and/or materials [31-37]. In the studies of some researchers, it is stated that it can contain a maximum of 18 materials in general, selected from a list of more than 2000 raw materials, especially for the creation of brake friction composite materials and the optimisation of their friction-wear behaviour [34-39]. Although brake pad friction materials used in the automotive industry are generally composed of three main matrices (metallic, semi-metallic/sintered and non-metallic) [11], ceramic [40] and carbon composites [41]. Brake friction materials generally consist of 4 different component parts depending on mechanical strength and manufacturing capability in order to fulfil the expected task. These are categorised as follows; reinforcement and filler, abrasives, friction modifiers and binder [2, 31, 32, 36, 42-46]. Although the selection of brake friction materials in these sections is usually based on good experience or trial and error applications, it involves tests involving long-term and detailed research in determining a new formulation of the composite to be formed [31, 33, 47]. For this purpose, each component in brake pad friction materials is selected with different precision. 'Binders' are used to provide mechanical resistance and maintain pad integrity during use as well as a thermally stable matrix, 'abrasives' are used to increase the coefficient of friction, improve wear resistance and control the formation of friction film, 'solid lubricants' are used to counteract the effect of deposition at high temperatures and stabilise the coefficient of friction, and 'reinforcements' are used to increase mechanical strength [48-54]. Thus, the brake pads developed or manufactured provide a sufficiently high coefficient of friction in contact with the metal disc. At the same time, it is also aimed that the coefficient of friction of the brake disc will not lose its performance at high temperatures and provide a constant coefficient of friction with the surface of the brake disc [31, 33, 47].

In essence, the expected characteristics of friction materials for brake pads include mechanical durability, appropriate thermal properties, a sufficient and stable friction coefficient depending on a wide range of operating conditions (including pressure, temperature, and environmental factors like dust, water, and ice-melting agents), high wear resistance, and good compatibility with anti-friction additives. Additionally, an ideal brake pad friction material is expected to operate reliably without contamination and noise in various conditions such as hot, cold, dry, or wet environments [9, 11, 55, 56]. Researchers developing friction materials for brake pads and conducting studies in this field prefer

materials and the percentage values by weight in the created composition, as presented in Table 2.1. The majority of friction materials for brake pads are generally considered organic. This is because the matrix of complex composites is formed by one or more organic polymers [9, 11].

Additionally, as a reinforcement material, both organic and inorganic fiber materials are supported [57, 58]. The preference for widely used organic friction materials is influenced by factors such as a simple preparation method, excellent tribological resistance, and environmental friendliness [57]. The environmental impact of brake pads in their operational use is profound. Brake pads release wear residues and toxic substances into the atmosphere due to wear, leaving negative traces on human health [58]. To reduce these negative effects, increasing the percentage of organic or inorganic additives in the brake pad composition can be considered beneficial for public health. The use of inorganic materials in brake pad friction materials is similarly effective. For recently planned alternative friction materials for brake pads, the use or preference of an inorganic "alkali-activated" material binder, which can completely harden when exposed to an alkaline environment (i.e., at high pH values), by leveraging the hydraulic activity of specific components would be effective [54, 59-62]. Therefore, the recent focus on using geopolymer materials provides incredible contributions to both human health (reducing respiratory problems) and the environment (reducing potential natural resource consumption and dust emissions into the atmosphere) [1].

Table 2.1. Materials used in brake pad friction materials and their average proportional values

<i>Composite Material Components</i>	<i>Materials used or R&D Studies</i>	<i>Average (%wt) Proportional Values</i>	<i>References</i>
<i>Binders (B)</i>	Phenolic Resin	% 7-25	[33, 37, 44, 46, 51, 63-65]
	Geopolymer	% 0-7	[33, 37]
	Condensed polynuclear aromatic resin (COPNA)	% 0-30	[37, 50, 66-69]
	Silicone modified phenolic resin	% 3	[37, 50, 70]
	Thermoplastic polyimide resin	% 5-10	[37, 50, 71, 72]
	Cashew nut shell liquid (CNSL)	% 0-10	[37, 64, 73]
	Forest Products	% 1-6	[37, 51, 65, 74]
	Thermoset resin	% 10-40	[37, 74, 75]
<i>(A+B)</i>	NBR	% 2.2 -3	[11, 41, 65, 76]
	SBR	% 10	[77]

Abrasives (A)	Iron oxide	% 0-8	[46, 78]
	Black Iron	% 0-5	[46, 78]
	Zirconium Silicate (ZrSiO ₄) Zirconium Oxide (ZrO ₂)	% 3-6	[46, 78]
	Aluminium Oxide (Al ₂ O ₃)	% 5-10	[79-81]
	h-Boron Nitride	% 0-10,5	[7, 33, 82, 83]
	Boron Carbide (B ₄ C)	% 10-20	[82, 84-86]
	Ulexite	% 4-12	[80]
Borax	% 4-12	[80]	
Boron Oxide	% 3-6	[78, 87]	
Boron	% 0,6-2	[88]	
Solid Lubricants	Graphite	% 3-15	[7, 37, 46, 48, 64, 89, 90]
	Metal Sulphide	% 0.5-10	[6, 37, 46, 48]
	Coke-carbon	% 5	[37, 51]
	Potassium titenate	%10-15	[36, 43, 44, 46]
	Iron powder	% 0-15	[73, 97]
	MoS ₂	% 5	[46, 52, 63]
Reinforcements and Fillers	Metal	% 0-20	[46, 48, 63, 91]
	Carbon	% 3-15	[46, 65, 82, 92]
	Glass fibre	% 5-30	[36, 43, 44, 46]
	Kevlar	% 0-30	[36, 43, 44, 46, 93]
	Mineral, ceramic fibres	% 4-10	[73, 76]
	Palm kernel fibres	% 10-40	[73]
	Coconut shell or fibres or powder	% 5-50	[66, 73, 94, 95]
	Periwinkle Shell	% 40-60	[96]
	Kaolin Mineral	% 25-40	[97]
	Ceramic	% 3.5-20	[46, 80, 82, 97, 98]
	Banana peel	% 5-30	[73]
Egg shell	% 3-18	[73]	
Mika	% 4,5-9	[6, 66]	
Vermiculite	% 0-10	[36, 43, 44, 46, 93]	
Barium Sulphate, Barite	% 6-50	[6, 7, 30, 46, 51, 90]	
Calcium Carbonate	% 10-15	[2, 99]	
Calcium Sulphate Crumbs	% 5-15	[65]	
Copper fibre, copper powder	% 6-12	[30, 43, 46,80,100]	
Brass fibre, Brass shavings	% 4-15	[36, 43, 44, 46, 80]	
Zinc	% 0-8	[90]	
Zircon	% 5-6	[36, 43, 44, 46]	

	Aramid fibre	% 0-30	[37, 46, 48, 65, 78]
	Rock wool	% 0-30	[37, 46, 48, 65, 78, 82]
	Steel wool	% 4-20	[37, 78, 96, 101, 102]
	Twaron fibre, Lapinus fibre	% 10	[63, 64, 93]
	Rubber Powder	% 2-4	[6]
	Wollastonite	% 6	[66, 70]
	Fly Ash	% 10-40	[89, 103, 104]
	Cashew Shell powder	% 5-10	[43, 44, 46]
	Hazelnut shell	% 7	[6, 105]

The use of geopolymer additives in brake materials aims to reduce the amount of phenolic resin, which releases volatile organic compounds (VOCs) when brake pads are exposed to temperatures exceeding 300°C during their functions [9, 106]. In a study conducted on this matter, Akmal and colleagues evaluated the effects of separately adding carbon fiber and sulfur to geopolymer-enhanced brake pad composites. Although brake pads reinforced with carbon fiber experienced a relatively slight decrease in the friction coefficient, it positively improved their mechanical strength. On the other hand, those with sulfur additives were noted to increase both the strength and friction coefficient. Consequently, it has been suggested that geopolymer composites with carbon fibers could serve as an alternative material to traditional brake blocks. This is because geopolymer composites offer top-level advantages such as being more cost-effective, lightweight, and heat-resistant compared to traditional brake blocks [107]. Furthermore, opting for an inorganic matrix instead of traditional organic-based binders not only benefits the high-temperature production process of brake pads but also contributes to overall energy savings in the total embodied energy of brake pads. This is achieved by considering both the production process and raw material selection, leading to a significant reduction in concrete energy consumption [54].

2.2. Production Methods of Brake Friction Materials

The initial process in producing the composite composition for brake pads is carried out after determining the materials and proportional contributions to be included in the content. Once these decisions are made, a mixing machine (such as ball milling, mixer, high-energy mixer, or electric blender) is used to ensure the macroscopic homogeneity of the materials. The mixing is performed within an average specific speed range (120, 2000, 3000 rpm) and for an average specific time (2-20 minutes) [41, 46, 63, 90, 93, 108].

In the subsequent step, the homogenized composite mixture is shaped into a specific form through cold or hot pressing, depending on the preferred production

application. The choice of the pressing method is determined especially by the type of material used and the resin type. Additionally, there is a processing condition known as hot pressing following cold pressing. The average molding pressures in cold pressing range between 80 bar and 150 bar, while for hot pressing, pressures are applied between 80 bar and 183.67 bar. The pressing processes for brake materials in molds are carried out within specific time frames. Particularly in hot pressing, both temperature and the active process are observed. In various studies, the temperature values during pressing ranged between 150°C and 180°C, and the time applied varied between 6 minutes and 15 minutes. Subsequently, the samples obtained from the pressing stage are subjected to firing for sintering. This process involves applying different temperature regimes, and the sintering of samples is performed at various temperature intervals. Therefore, they exposed the samples to different time durations under various temperature applications for the sintering process [7, 30, 63, 76, 77, 80, 93, 96, 98, 109, 110].

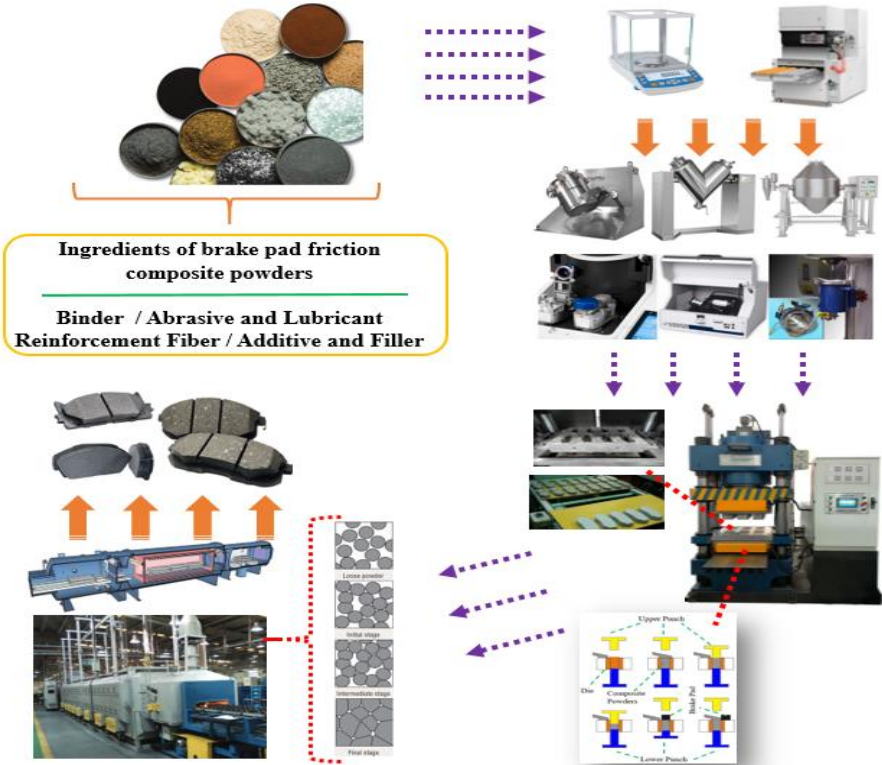


Figure 2.1. Sequential Manufacturing Steps in the Production Process of Brake Pads [111-127]

When examining studies conducted at different temperature stages, Mahale et al. (2019) subjected their brake pad samples to treatment at two different temperatures, namely 120°C and 160°C, for 2 hours and 5 hours, respectively. Kosbe et al. (2020) conducted a study with four different temperature levels, namely 150°C, 250°C, 450°C, and 550°C, applying the treatment for all at the same duration of 30-minute intervals. Jeganmohan et al. (2020) performed a curing process for brake pad samples at a constant temperature of 120°C for 6 hours. In their study, Cai et al. (2015) exposed their produced brake pad samples to curing processes at five different temperature levels, namely 120°C, 140°C, 160°C, 180°C, and 200°C, with respective sintering times of 1 hour, 1 hour, 1 hour, 2 hours, and 1 hour. Singh et al. (2023) conducted a curing process for their manufactured brake pads at a constant temperature of 170°C for 4 hours. Yang et al. (2020) subjected their brake pad samples to a curing process at a constant temperature of 150°C for 4 hours. Generally, after the samples are removed from hot pressing, they are subjected to an average curing process at a constant temperature of 150°C for 4 hours [2, 7, 41, 63, 65, 90, 93].

3. Geopolymers and Production of Geopolymer Additive Brake Friction Materials

3.1. Geopolymers

The polymers known as geopolymers are mostly composed of aluminosilicate-based inorganic polymers and are included in geochemically derived polymers [128-131]. Geopolymers are also referred to as inorganic polymer glass, alkali bonded ceramics and hydro-ceramics. [132]. The depth under the name geopolymer that Davidovits deems appropriate is that the reaction that occurs during the formation of geopolymer is similar to the polycondensation (polymerization reaction) reaction of thermosetting (hardening on heating) polymers [133]. Geopolymers are the ultimate products of a chemical process that occurs through the combination of geological formations containing amorphous aluminosilicate and powdered binders (such as ground granulated blast furnace slag, waste materials like fly ash, and calcined kaolin clay, namely metakaolin) in an alkaline environment (comprising sodium or potassium-based components, such as potassium hydroxide and potassium silicate or a mixture of sodium hydroxide and sodium silicate). In addition, it is indicated that ions such as Li^+ and Ca^+ can provide an alkaline environment or can be utilized in acidic conditions, such as phosphoric acid and humic acid [18, 134-138]. In this process, the progression of polymerization with the formation of Si-O-Al and Si-O-Si covalent bonds in the chemical reaction in alkaline environment and thus the development of 3-D polymer chain takes place. Additionally, the inclusion and utilization of waste materials like fly ash and slag contribute to both recycling and the reduction of greenhouse gas emissions [133, 135, 136, 139]. Figure 3.1 shows the impact of Si/Al molar ratio on alumina glycate chain alignments in the formation of geopolymer form. According to Davidovits, who has carried out detailed studies in the field of geopolymers, it was indicated that geopolymers are polymeric three-dimensional silicon-oxygen-aluminium materials containing a large number of amorphous and semi-crystalline phases [18]. In other words, aluminosilicate materials used in geopolymer production in the presence of alkaline environment produce a structure ranging from amorphous to semi-crystalline by geopolymerisation reaction [140].

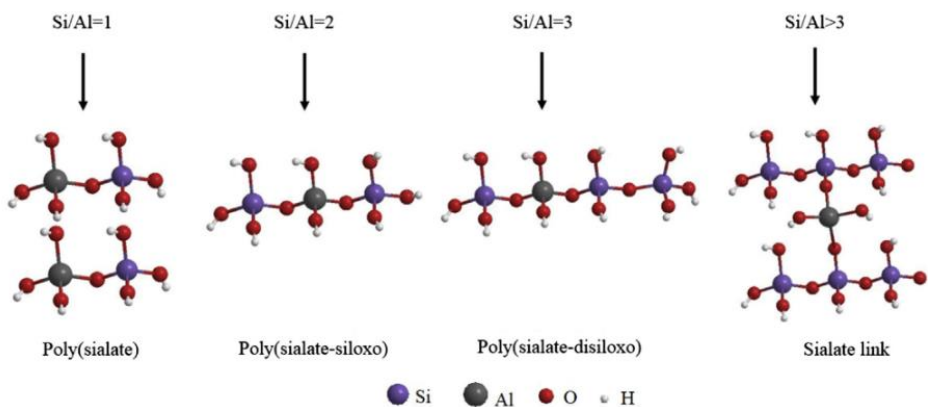


Fig. 3.1. The impact of Si/Al molar ratio on the alumina-silicate chains in the formation of geopolymer structure [141-142]

For geopolymers synthesised by tetrahedral polycondensation of SiO_4 and AlO_4 in aqueous solution [18], it is emphasised that the negative charge of AlO_4 tetrahedra should be balanced with the support of positive ions (Na^+ and K^+) in the system in order to have a stable structure [18, 143, 144]. In the geopolymerisation process, raw materials containing aluminosilicate dissolve in alkaline solutions, leading to the formation of aluminate and silicate monomers. These monomers are transformed into oligomers (small polymer group containing much less monomer than polymers) and then into geopolymers. The gradual process stages in which the geopolymerisation process is applied include dissolution, reorganisation or reorganisation, condensation and polymerisation processes. Dissolution and reorganisation form many oligomer forms. Oligomers bond to form large polymer chains. When oligomers bind, they release water by sharing an oxygen atom with OH groups. In this context, the stages of the geopolymerization process are depicted in Figure 3.2 [138].

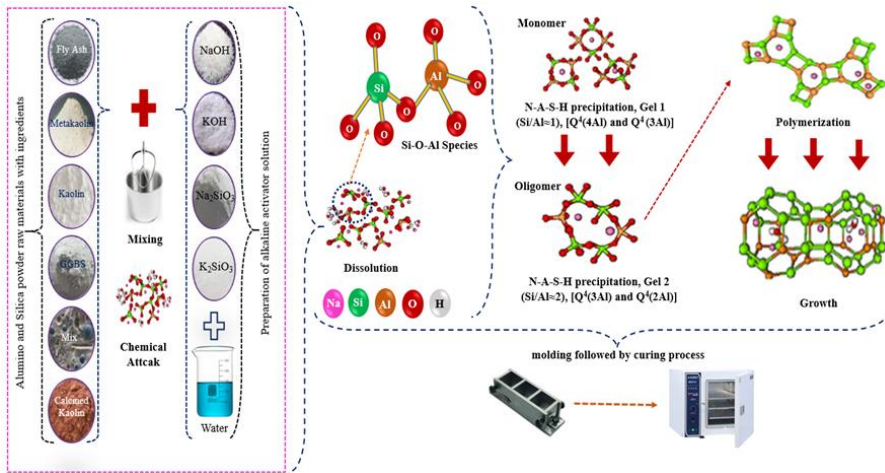


Figure 3.2. Visualization of the stages of the geopolymerization process [145-150]

In a comprehensive assessment, it is observed that the structural distinctions and resulting characteristics of geopolymers are influenced by various factors, not only during synthesis but also by the aluminosilicate material (type, surface area, glassy phase content), alkali solution/aluminosilicate ratio, H_2O/Na_2O molar ratio, water/solid material ratio, Na_2O/SiO_2 ratio, SiO_2/Al_2O_3 ratio, alkali metal cation type and concentration, curing type, and curing regimen (temperature and application duration). These parameters are recognized as influential factors shaping the properties of Geopolymers [144, 151, 152]. The two groups of components, alkaline activators and aluminosilicates, which are the basis for the synthesis of geopolymers are presented in table 3.1.

In the production of geopolymers, alkali activators are commonly utilized in the forms of hydroxide and silicate solutions. Among these, potassium hydroxide (KOH) and sodium hydroxide (NaOH) are extensively employed as alkali hydroxide activators. Both potassium hydroxide and sodium hydroxide contribute to the formation of the crystalline zeolite structure. Crystallization is most prominent in the rapid utilization of sodium hydroxide. It is crucial to note that the high corrosive nature of alkali hydroxide activation and the release of high temperatures during dissolution (the temperature can rise up to $90^\circ C$ with a 10 molar sodium hydroxide solution) underscore the importance of considering its non-user-friendly aspects. Another disadvantage in alkali hydroxide solutions is illustrated by the increased viscosity with rising molarity [153].

Table 3.1. Sources of aluminosilicate and alkaline activators [138, 153]

<i>Aluminosilicate Source</i>	<i>Alkaline Activators</i>
<ul style="list-style-type: none"> ▪ <i>Fly Ash</i> ▪ <i>Blast furnace slag</i> ▪ <i>Metakaolin</i> ▪ <i>Red Mud</i> ▪ <i>Silica Fume</i> ▪ <i>Palm oil Ash</i> ▪ <i>Rice paddy Ash</i> 	<ul style="list-style-type: none"> ▪ <i>Sodium hydroxide (NaOH)</i> ▪ <i>Sodium silicate (Na₂SiO₃)</i> ▪ <i>Potassium hydroxide (KOH)</i> ▪ <i>Potassium silicate (K₂SiO₃)</i> ▪ <i>Calcium hydroxide (Ca(OH)₂)</i> ▪ <i>Other silicates (LiOH (Lithium Hydroxide), RbOH (Rubidium Hydroxide) and CsOH (Cesium Hydroxide))</i>

Davidovits (2017) proposed the structural model shown in Figure 3.3 for geopolymers produced using potassium alkali ion.

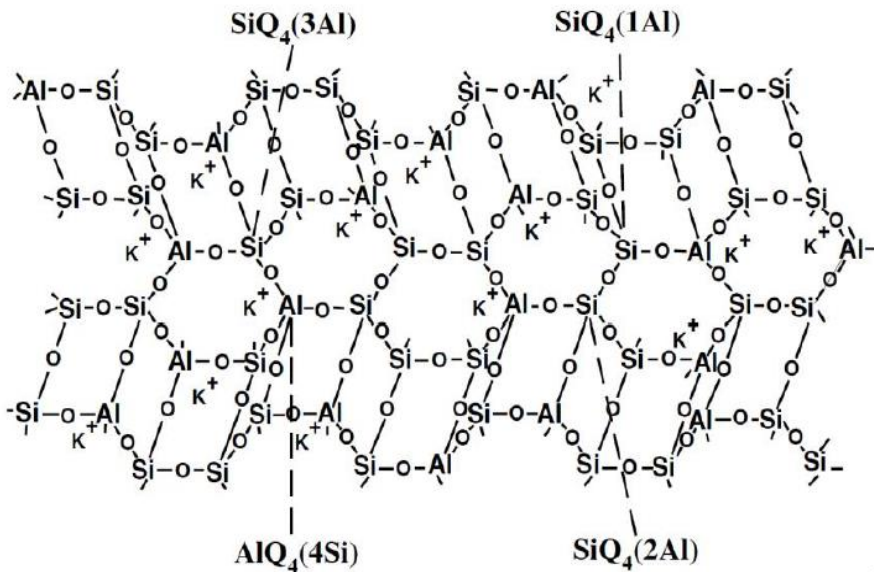


Figure 3.3. Microstructure after geopolymerisation [129]

Alkali silicate solutions contain Na₂O or K₂O, combined with Si₂O and water mixtures. It should be noted that dissolved silica (silicon dioxide or SiO₂) is somewhat acidic. Silica can be exemplified as monomeric silica and behaves as a weak acid under alkaline conditions. Therefore, the pH of the silicate activating solution is buffered between 11-12. The viscosity of the alkali silicate activator is known to increase with the Si/Na ratio. Sodium silicate is the most commonly used silicate activator in the geopolymerization process [154].

Aluminosilicate-based materials, which are prominently featured as primary components in the production of geopolymers, play a crucial role. As indicated in Table 3.1, key materials used in production include fly ash, blast furnace slag, metakaolin, red mud, silica fume, palm oil ash, and rice husk ash. Additionally, the combination of volcanic tuff, kaolin, calcined minerals, and non-calcined materials is also positioned as compatible materials within this category [155, 156]. There are 10 different classes of geopolymer materials, influenced by the raw materials used and the Si/Al ratio in their composition. The contents of these materials are presented in Table 3.2.

Table 3.2. Variations Among Different Classes of Geopolymer Materials [157]

1	Waterglass-based geopolymer, poly(siloxonate), soluble silicate, Si:Al=1:0
2	Kaolinite / Hydrosodalite-based geopolymer, poly(sialate) Si:Al=1:1
3	Metakaolin MK-750-based geopolymer, poly(sialate-siloxo) Si:Al=2:1
4	Calcium-based geopolymer, (Ca, K, Na)-sialate, Si:Al=1, 2, 3
5	Rock-based geopolymer, poly(sialate-multisiloxo) $1 < \text{Si:Al} < 5$
6	Silica-based geopolymer, sialate link and siloxo link in poly(siloxonate) Si:Al>5
7	Fly ash-based geopolymer
8	Ferro-sialate-based geopolymer
9	Phosphate-based geopolymer, AlPO ₄ -based geopolymer
10	Organic-mineral geopolymer

It is stated that the aluminosilicates generally preferred in geopolymer production are fly ash, ground blast furnace slag and metakaolin. Among these aluminosilicate based materials, fly ash is a by-product of coal combustion defined as pulverised fuel ash and is known to have a low calcium chemical property. When evaluated mechanically, fly ash doped geopolymer materials, which have high strength, are characterised to have a long fatigue life and low cost due to their low permeability. When the chemical composition content of fly ash doped geopolymers with Si/Al ratio = 2 is examined, silicon (Silicon: SiO₂) and aluminium oxide (Al₂O₃) values constitute 80% by mass. Iron oxide (Fe₂O₃) ratios in fly ashes generally vary between 10% and 20% by weight, while the presence of calcium oxide (CaO) is less than 5% by weight. The carbon content is less than 2 wt% in the light of the design determination of the loss on superheating. The use of fly ash also has a positive effect on land area conservation, water reduction, energy consumption and dealing with environmental problems such as greenhouse gas effects. The overall average size and blain surface area of fly ash particles are 9µm and 0.37 m²/g, respectively. Thanks to this very small particle structure of fly ash, it increases the density of

geopolymer structured products and makes it effective to be resistant to freezing [154].

Ground blast furnace slag (YFC), which is in the aluminosilicate family, is a by-product like fly ash and is produced by burning iron ore, coke and limestone mixtures for iron production at 1500°C. The composition of the slag taken from the casting surface in molten form is approximately 40 % CaO (calcium oxide) and 30%-40% SiO₂ (silicon dioxide). Furthermore, in geopolymer production, the aluminium and silicon contained in the slag are activated by a mixture of sodium silicate and sodium hydroxide solutions to produce a binder-like geopolymer paste [154]. Due to its contribution to early hardening in geopolymer production, it can offer the advantage of demoulding after about 1 hour. The addition of calcium compounds has two main effects, the first effect is the improvement of C-S-H or/and C-A-S-H formation and activation, and the second is the effect of a calcium cation (Ca²⁺) acting as a charge stabilising cation [158]. Especially in geopolymer concretes, some advantages can be obtained when slag is preferred over Portland cement. These advantages are high compressive strength, resistance to high temperature and chemicals. The reason why YFC-added geopolymer concrete is more advantageous against Portland cement against high temperature is that more cracks may occur in Portland cement when exposed to high temperature. As a result of the studies, it was observed that geopolymer concretes maintained their compressive strength up to 400°C. The reason for this is that the alumino silicate material formed by alkaline activators used in geopolymer concretes shows better resistance to heat [159]. In a conducted study, it has been noted that although the inclusion of slag significantly enhances the mechanical performance of fly ash-based geopolymer mortars (with compressive strength exceeding 100 MPa), it adversely affects their high-temperature performance. Furthermore, control geopolymer mortars (produced solely with fly ash) exhibit approximately 90% of their initial strength at 1000 °C, making them recommended for use in structural elements exposed to high temperatures [160]. Lastly, among the raw materials, metakaolin, which is the calcined form of the clay kaolinite, representing its dehydroxylated state, is an effective and commonly used material as a pozzolanic reactive substance. The advantage of using metakaolin in geopolymers lies in its ability to control the Si/Al ratio, its white color, and high solubility in an alkaline solution. However, using metakaolin as a source material in geopolymers is expensive because it requires calcination at temperatures around 500°C - 700°C [155, 161].

Today, metakaolin serves as a commonly used binder in geopolymer concrete and mortar due to its ability to rapidly gain strength and form a strong bonding mechanism with alkali-activated solutions [162-164]. Davidovits extensively

investigated materials with pozzolanic characteristics for their binder properties in geopolymer production. According to the results, metakaolin-slag-based geopolymers are recognized as the best composites in terms of both environmental friendliness and mechanical and durability performance [165, 166]. The dehydroxylated form of kaolinite is now referred to as MK-750. Here, MK stands for metakaolinite, and 750 indicates the calcination temperature of 750°C [167]. Davidovits' patent (1982) focuses on the IV coordination number of Al in dehydroxylated kaolinite. The significant aspect of Davidovits' (1978) and Leonard's (1977) updated research on the structural analysis of dehydroxylated clay minerals (kaolinite) using radial electron density distribution and X-ray spectroscopy lies in the examination of the amorphous or weakly crystallized phase of metakaolinite obtained at 600-800°C. The structure of dehydroxylated kaolinite is illustrated in Figure 3.4 [167].

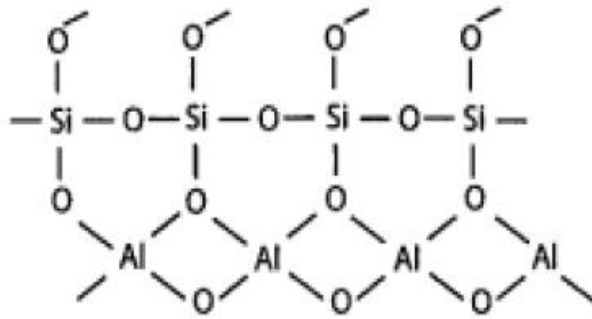


Figure 3.4. Structure of dehydroxylated kaolinite [167]

Pelisser et al. examined the mechanical properties of metakaolin geopolymer mortars in their study. Experiments were conducted to determine the elastic modulus, hardness, compressive and flexural strength, flexural modulus, and microstructural analysis. The results demonstrated that geopolymer mortars outperformed Portland cement mortars in terms of strength properties and elastic modulus. Additionally, both geopolymer and normal Portland cement mortars exhibited similar micromechanical properties, but geopolymer mortars showed better deformation capacity and tensile strength [168].

Rovnaník conducted experiments on the effect of curing temperature on the hardening development of metakaolin-based geopolymer structures. The study aimed to investigate the impact of curing temperature (10, 20, 40, 60, and 80°C) and duration on compressive and flexural strength, pore distribution, and the microstructure of alkali-activated metakaolin material. The research revealed a relationship between increasing pore size and cumulative pore volume with rising

temperature, affecting the mechanical properties. Additionally, it was concluded that monitoring the reaction process was possible through Infrared Spectroscopy experiments [169].

Lahoti et al. evaluated the influence of Si/Al (molar ratio), water/binder (mass ratio), Al/Na (molar ratio), and H₂O/Na₂O (molar ratio) on the compressive strength of metakaolin-based geopolymers. The research findings indicated that the Si/Al ratio, followed by the Al/Na ratio, was the most significant parameter, and unlike normal Portland cement, the water/binder ratio was not the most critical factor affecting the strength of metakaolin-based geopolymers [170].

Zhang et al. conducted an experimental study on geopolymers binders composed of a mixture of metakaolin and fly ash, specifically developed for fire resistance applications. Flexural and compressive tests were conducted at room temperature and after exposure to high temperatures. The development of an optimal MK-FA mixture was possible based on mechanical properties and thermogravimetric analysis results. A geopolymer based on MK-FA was considered a potential alternative to traditional Portland cement in practical construction categories [171].

3.2. The Practical Applications of Geopolymers

Over the past thirty years, diverse applications in various fields of technology, encompassing geopolymers, have been proposed and utilized. The material properties, along with the components involving their processing methods, have shed light on potential applications in versatile areas and numerous industries, offering high-level contributions. Geopolymers, with their minimal CO₂ emissions, low energy consumption, low production costs, and rapid strength gain, find applications in advanced construction materials, fire-resistant materials, refractories, and stabilization of hazardous waste.

However, with the developed scientific foundation and research and development support, their incorporation into alternative engineering fields is surpassing their existing and proven characteristics. Their advanced mechanical, thermal, and chemical properties, as well as potentially higher durability, make them effective in various engineering applications. Geopolymers and their derivatives, with superior performance advantages, have found their place in engineering fields, primarily in construction but also in automotive, aerospace, metallurgy, and the plastic industry. Geopolymer composites, showcasing functional inclusiveness, serve in applications such as rapid setting and strength gaining, making them materials used for fast repairs on airport runways, among other purposes. Among other construction applications, the use of geopolymers extends to the production of bricks, tiles, railway sleepers, box culverts, wall

panels, and prefabricated products like pipes. The common practice in these products involves the use of particulate or short fiber binders. For low-tech building applications, inexpensive organic fibers such as wool, flax, or paper can be used in the production of geopolymer composites. Geopolymer composites with organic fibers are inherently fire-resistant due to the inorganic geopolymer matrix. Numerous studies indicate the use of geopolymer composites for mold and tool materials, operating at high temperatures. Table 3.3 presents the recommended areas of use for geopolymers based on the Si/Al ratio in various fields [15-17, 172, 173].

Table 3.3. Recommended application areas for geopolymers based on their Si/Al ratios [173]

Si/Al	Application Areas of Geopolymers
1	In bricks, ceramics, and fire protection products
2	Low CO ₂ cement, concrete, and in the storage of radioactive waste
3	Heat-resistant materials, glass fiber products
>3	Industrial products that provide sealing
20<Si/Al<35	Materials resistant to fire and heat

Geopolymer composite-derived materials combine good tolerance sensitivity and the reproduction of surface details with lightweight; they are cost-effective, easy to prepare and repair, and do not require high-temperature production techniques, thus providing ease of on-site construction with rapid curing. Beyond applications in the construction sector, they have been reported to be used in the aerospace industry for the production of composite components and in the refractory industry for metal casting [16-18], as well as in insulation and fire protection for buildings [147]. Concerns about temperature or fire safety, when there is resistance to the widespread use of organic polymer composites, lead to the preference for fiber-reinforced composite panels. For this purpose, the creation of flame-resistant smokeless interior linings for aircraft, successfully implemented with geopolymer composite panels [18], or as heat shields in high-performance race cars [17, 21], has been achieved.

With the evolving preference for geopolymer use, it has also found its place in the automotive industry, particularly in a significant area such as brake pads. The presence of environmentally harmful materials in brake pad materials has been known for years, keeping research on this issue continually relevant. Brake pads made with asbestos fibers, which can be harmful to the human population and the environment, are known to turn into toxic dust during braking and be released into the air with the wind. Because these toxic dust particles are believed

to contain many hazardous substances, they can potentially harm human respiration and skin [1, 9, 130, 174]. For eco-friendly brake materials, the development of new-generation derivatives using geopolymer matrix and natural fiber waste, which can replace phenolic resin and synthetic fibers, is being pursued. Both the binding resin and reinforcement fibers are reported to significantly contribute to the friction properties of the produced material [37, 175-178]. Additionally, standard traditional brake pads such as semi-metallic and ceramic brake pads are quite expensive. Therefore, the use of geopolymer brake pads is envisioned to reduce the production cost of brake pads in the automotive industry [1].

3.3. Mechanical Properties of Geopolymer Materials

In the mechanical behavior of materials, loadings, temperature, and interactions with the environment are functionally comprehensive. In many practical problems, the combined effects of these control parameters are evaluated. However, before attempting to understand the combined effects of load and temperature or the effects of load and environment, the individual effects of loads (elastic and plastic deformation) should be detailed and assessed. Material response can also depend on the nature of the loading. When deformation applied continuously increases over time (as in tensile testing), reversible (elastic) deformation can occur at lower loads before irreversible/plastic deformation begins at higher loads. Under reverse loading, the material can also undergo a phenomenon known as "fatigue," which occurs even at stresses below those required for bulk plastic deformation. Fatigue can lead to destructive fractures if not anticipated in the design of most engineering structures and components [179]. Thus, in determining the mechanical property of the material, the change in all these parametric effects should be considered for necessary designs and evaluations. Therefore, it can be said for geopolymers as well that they are expected to have good durability in terms of mechanical properties before being used in some engineering structures or products.

Research worldwide on geopolymers with composite content has revealed extraordinary benefits in terms of mechanical strength, resistance to high temperature, wear, water absorption, etc. [180]. In evaluating the mechanical properties of geopolymers, the matrix structure and the general composite form are considered in two separate ways. When looking at the mechanical properties of the geopolymer matrix, it depends on the nature of alkali cations in the structure as they balance the negative charge associated with tetrahedral aluminate units combining with silicate units to form a three-dimensional structure [17, 19, 20]. The mechanical properties of materials made with

geopolymers are influenced by the following parameters: (a) the ratio of alkali activator solutions to source (precursor) materials (fly ash, metakaolin, etc.), (b) the molarity of sodium hydroxide solution, (c) the SS/SH ratio, which is also dependent on the composition of SS, (d) curing temperature, (e) curing time, (f) water content [141, 181]. When evaluating the reported mechanical measurements, they are mostly based on comparison with cement. Here, the assessment of the effect of compressive strength after varying curing times becomes crucial. The source of aluminosilicate and reaction conditions significantly affect the compressive strengths of geopolymers. This controls the strength of the gel phase, the ratio of the gel phase to unreacted Al-Si particles, the nature of the amorphous phase, the degree of crystallinity (or its absence), and any surface reactions between the gel phase and unreacted particles [20, 182].

Ferone and colleagues conducted a study on the impact of the $\text{SiO}_2/\text{Na}_2\text{O}$ ratio on the mechanical properties and microstructure of metakaolin-based geopolymer mortar. They prepared four geopolymer mixtures with various molar ratios ($\text{SiO}_2/\text{Na}_2\text{O}$). The curing time of the mixtures was seven days at room temperature with 100% relative humidity. It was found that the $\text{Si}/\text{Al} = 1.75$ ratio is a balanced ratio that improves the mechanical properties of the mixtures and reduces shrinkage. Mixtures with high Si/Al ratios are more likely to experience drying shrinkage issues due to high capillary water absorption resulting from the evaporation of water. They also noted the presence of larger-sized pores in samples with lower Si/Al ratios [183]. Therefore, the evaluation of the mechanical strengths of alkali-activated materials depends on the design of the applied mixture (Si/Al , Al/Na , water/ Na ratio, etc.) and the reactivity degree of the components [184].

Rodríguez and others [185] achieved optimum compressive strength with a 1.5 Si/Al ratio. The study observed that increasing the Si/Al ratio allowed for an increase in compressive strength without any loss in strength, compared to lower Na/Al ratios that significantly reduced strength when the Si/Al ratio exceeded 1.75. Subaer examined the effect of changing the Na/Al ratio on the visible porosity of geopolymers and compared these results with compressive strength results. They observed an inverse relationship between the two, implying that porosity to some extent controls compressive strength since higher porosity results in lower compressive strength. In this study, higher strength was obtained at $\text{Si}/\text{Al} = 1.5$, and compressive strength values decreased afterward. The results also indicated that an increase in Na content led to a decrease in compressive strength in geopolymers. Yunsheng and colleagues [186] achieved a simple compressive strength of 34.9 MPa with a Si/Al ratio of 2.75, Na/Al ratio of 1, and $\text{H}_2\text{O}/\text{Na}_2\text{O}$ ratio of 7.

Welter and MacKenzie investigated the mechanical properties of dehydroxylated kaolinitic clay activated with sodium silicate and NaOH solution. They found that a 50% reduction in NaOH content decreased both compressive strength and elastic modulus [17].

The effects of curing conditions on the flexural and compressive strengths and microstructures of metakaolin-based geopolymer were examined by Chen et al. [187]. Samples were cured at different temperatures (20°C, 40°C, 60°C, 80°C, and 100°C) and different curing times (24 hours, 72 hours, and 168 hours), with 50±5% relative humidity applied in the first 12 hours. The results showed that the best compressive strength was achieved in samples cured at 60°C for 168 hours because increasing the curing temperature accelerated the dissolution of aluminosilicate, thereby accelerating gel formation. However, high curing temperature resulted in a loss of moisture required to complete the geopolymerization reaction. Additionally, Rovnanik [188] investigated the effects of temperature and curing time on the mechanical properties of metakaolin-based geopolymer samples at 1, 3, 7, and 28 days. The silicate modulus of sodium silicate was 1.39. Samples were cured at different temperatures (10°C, 20°C, 40°C, 60°C, and 80°C) for 4 hours and then stored at room temperature (20°C) with 45% humidity. It was found that increasing the curing temperature accelerated the structure formation in the early stages of the reaction. However, rapid setting constraints prevented the mixture from achieving a compact consistency. Conversely, samples cured at low temperatures showed a delay in strength development, achieving the target strength at 28 days. This was attributed to an increase in compressive strength with temperature due to the increased geopolymerization products in the early stages. However, at later ages, the quality of geopolymerization products becomes the dominant factor. Geopolymer develops slowly at low temperatures and later exhibits better quality in terms of porosity and compaction.

In Table 3.4, which essentially includes different components and ratios to form the geopolymer composite structure, the impact of these components and ratios on compressive strength is presented. In the analyzed studies, the Si/Al ratio generally ranged from 1.5 to 2.45, with values close to 2 often resulting in the highest compressive strengths. The Na/Al ratio varied between 0.75 and 1.2, with 1.0 being the most commonly used ratio. The H₂O/Na₂O ratio of 11 was frequently employed by the majority of the authors. It should be noted that the obtained mechanical strength indicators are also dependent on other parameters, such as the source of aluminosilicates and the manufacturing method of geopolymeric mixtures.

Table 3.4. Effect of Proportional Values in the Mixture on Mechanical Strength [184]

Material Source	Ratio Si/Al Optimal	Na/Al Ratio	H ₂ O/Na ₂ O Ratio	Application Conditions or Sample Size	UCS Strength [MPa]	Reference
Fly ash	1.87	1.2	11	Mech. mix. : 8 min Vibration for air removal. Cured at 80°C for 24 h.	88	[189]
Metakaolin	1.9	1	11	Mech. mix. : 15 min Vibration: 15 min Cured at 40°C for 20 h.	75	[190]
Metakaolin	1.9	1	11	Mech. mix. : 10 min Vibration for air removal. Cured at 25–30°C for 24 h.	81.6	[170]
Metakaolin	1.9	0.75 (K/Al:0.25)	11	Mech. mix. : 15 min Vibration: 15 min Cured at 40°C for 20 h. 28 days of rest at ambient conditions	95	[191]
Coal gangue, blast furnace slag and lead-zinc tailings	2.0	--	27% (water/solids)	Mixed and vibrated for 5 min. Cured at 30°C.	91.13	[192]
Red mud and fly ash	2.45	0.8	30% (water/solids)	Mech. mix. : 5 min Cured at 60°C for 24 h.	38	[193]

Iron ore tailing	5.98	--	--	Mech. mix. : 6 min Cured at 80°C for 24 h.	34	[194]
%50 GGBS+ %50 VA	--	0.76	37.5% (water/solids)	Mech. mix. : 10 min Vibration: 2 min Cured at 60°C for 24 h.	105	[195]
Metakaolin	1.5	0.75	12 (H ₂ O/Na ₂ O)	Mix. for 12 min. Vibration for 5 min. Rest in airtight container for 7 days with relative humidity of 90%.	35	[185]

It has been reported that the alkali activation of metakaolin with sodium silicate solution plus NaOH produces better compressive strength compared to samples activated solely with NaOH [20]. Therefore, the compressive strengths of geopolymer matrix materials cover a wide range, from 1 MPa for poorly formed products of solid-state synthesis [196] to 26 MPa for sol-gel synthesized geopolymers [197], and up to 110 MPa for a product synthesized from volatile ash activated with sodium silicate and NaOH solution [198]. Under the same conditions, geopolymerized metakaolin activated with NaOH has been reported to have compressive strengths of 15 MPa, 35 MPa for volatile ash, and 70 MPa for ground granulated blast furnace slag (GGBS). However, in another study, the compressive strengths of geopolymers prepared from GGBS activated with sodium silicate and NaOH were dependent on the concentration of NaOH, reaching a maximum value of 45 MPa when 8 M NaOH was used. In a study where metakaolin was added, a GGBS product activated with sodium silicate and KOH reported higher compressive strength; the strength of this material is 79 MPa. Although there are numerous compressive strength values available for geopolymer matrix materials, data becomes sparser when it comes to bending strengths and elastic properties, which are more intriguing in the context of fiber-reinforced composites [17, 199].

All geopolymers, being inorganic materials that demonstrate thermal stability, have melting points and crystallization products depending on the chemical composition of the raw material and the activating alkali used. According to the phase diagram for the SiO₂-Al₂O₃-Na₂O system, sodium geopolymers in this system should crystallize as nepheline (NaAlSiO₄) at approximately 1100°C,

even though the full crystallization temperature (and melting temperature) depends on the composition [200]. When heated, the corresponding potassium geopolymer forms crystalline leucite (KAlSiO_4), but it has been reported that the melting point of the potassium geopolymer is unusually high, approximately 1300°C [201]. On the other hand, in another study, leucite (KAlSi_2O_6) was found to be the primary phase above 1100°C , with only a small amount of leucite forming. Geopolymers based on metakaolin containing cesium were reported to be more refractory than those containing sodium and potassium compounds, as they crystallized pollucite ($\text{CsAlSi}_2\text{O}_6$) upon gradual heating [202]. Formulations of volatile ash-based geopolymers with very high thermal expansion in the $700\text{-}800^\circ\text{C}$ temperature range have been reported to have weak mechanical strength [203].

Geopolymers have been embraced as fire-resistant components in buildings and vehicles due to their superior thermal properties compared to Portland cement products. A 10 mm thick geopolymer panel synthesized from GGBS and KOH-activated metakaolin withstood temperatures of 1100°C for over 30 minutes, and the temperature increase on the opposite side was only 250°C [204]. The ability of geopolymers to provide thermal protection to embedded carbon fiber reinforcements has led to the use of these panels in the bodies of Formula 1 race cars, where they could withstand temperatures above 700°C for more than 3 hours [205].

The impact of slag on mechanical and microstructural properties has been investigated by Soleimani et al. [206]. The study involved the substitution of metakaolin with phosphorus slag at different weight percentages (10-100). The $\text{SiO}_2/\text{Al}_2\text{O}_3$ molar ratio was 0.8, and the solid ratio (liquid/solid) was 0.53, with curing performed at room temperature. The study concluded that the optimal substitution rate of slag for metakaolin is 40% by weight, resulting in a 14.5% increase in compressive strength at 28 days. The coexistence of both geopolymer and C-A-S-H gels contributed to an enhancement in mechanical strength. However, the study also observed a decrease in compressive strength due to the precipitation of C-S-H within the first 7 days and the lower amount of formed geopolymer gel.

Bernal et al. [207] investigated the thermal characterization of metakaolin/slag-based geopolymers. The study employed different Si/Al molar ratios and various slag/(slag + metakaolin) ratios. Curing was conducted at 60°C with more than 90% relative humidity for 24 hours. Samples were exposed to elevated temperatures (200, 400, 600, and 1000°C), and the remaining compressive strength after thermal exposure was measured. Results indicated that structural alterations in slag-enriched products compared to pure metakaolin

binders might require elevated temperatures. However, the unblended system exhibited higher residual compressive strength after exposure to 1000°C due to the reduction in alumina silicate glass resulting from the combination of geopolymers and calcium C-S-H gel formation caused by the geopolymers' reaction at 1000°C.

Despite offering numerous advantages, geopolymers are limited in applications due to their brittle nature. To overcome this limitation, reinforcing the matrix with fibers is a commonly preferred method due to its effectiveness and cost efficiency [208].

In fiber-reinforced composites, fibers exhibit a restrictive effect before cracking and mitigate brittleness through bridging capabilities after cracking [209]. They alter fracture behavior, increase tensile and flexural strengths, and significantly improve toughness properties [208]. Various researchers have frequently used different fibers such as polypropylene, carbon, basalt, PVA, glass, and steel to enhance the mechanical properties of geopolymers [17, 210].

Reinforcing fibers gradually take control of the mechanical properties of the composite as the fiber content increases, while thermal properties are primarily controlled by the matrix composition. Geopolymer matrices have demonstrated successful protection against combustion when carbon fibers are used, allowing the use of carbon fiber-reinforced composites in high-temperature oxidative environments [205, 211]. In addition to the complications arising from the variability in matrix compositions and processing parameters, comparing the properties of these composites becomes more complex due to the lack of standardized test methods and sample sizes used in various reported studies. Significant differences in aspect ratios and absolute dimensions of samples, especially in the open-depth ratios, can lead to dramatic changes in failure modes. Moreover, insufficient explanation of fiber sizing and content in many old publications (as well as in some new reports) hinders valid comparisons between studies. Fiber sizing is particularly crucial since it significantly alters the failure behavior of a composite. For this purpose, the fiber structure within a composite can vary in normal, discrete or chopped forms, and unidirectional forms, leading to variations in mechanical properties. The main advantage of discontinuous fiber-reinforced composites is their relatively easy manufacturing and reasonable improvement in mechanical properties [17].

Behera et al. [212] examined the properties of basalt microfibril geopolymers when exposed to high temperatures (200°C, 400°C, and 800°C). Three different proportions of basalt microfibrils were added to the geopolymer mixture (5%, 10%, and 15% by weight), and curing was carried out at room temperature (20°C) for 28 days with a relative humidity of $\pm 10\%$. Geopolymer with added basalt

microfibrils exhibited higher compressive strength than fiberless geopolymer. The improvement in strength of fiber-reinforced samples was attributed to the denser microstructure in the paste due to the effect of basalt microfibrils on the strength development. However, an increase in temperature up to 200°C resulted in enhanced strength due to the dehydration shrinkage of the geopolymer caused by the evaporation of free water at 200°C. The study suggested that basalt microfibril-enhanced geopolymers could be suitable for high-temperature applications in thermal coatings.

Midhun et al. (2018) conducted a study on the fracture behavior of geopolymers containing glass fibers. The research utilized a mixture consisting of 70% Class F fly ash, 30% blast furnace slag, activated with an activator solution with a sodium silicate/sodium hydroxide ratio of 2.5. Coarse aggregate was granite, and fine aggregate was river sand. Geopolymer concretes were produced, with one being a control mixture without fibers and eight fiber-reinforced concretes containing alkali-resistant glass fibers of 6 or 13 mm length at volumetric ratios of 0.1, 0.2, 0.3, and 0.4. Experiments were conducted on notched specimens of dimensions 100x100x500 mm using a single-point bending test setup in a displacement-controlled machine with a loading rate of 0.2 mm/minute. Fibers were added to the mix along with other materials, mixed using a mixer, and flexural strengths were determined on specimens of size 100x100x500 mm using a two-point loading test setup. Notched specimens had notch depth ratios of 0.1, 0.2, and 0.3. Researchers reported an increase in flexural strengths in all fiber-reinforced samples, with increases ranging from 52.4% to 57.1% for concrete with 6 mm and 13 mm fibers, respectively. Additionally, an increase in fiber content resulted in elevated displacements and fracture energies for all notch depth ratios, with increases ranging from 15.2% to 48.9% at 7 days and from 10.6% to 39.4% at 28 days. It was also reported that steel fiber addition increased toughness values by 84.5%, 172.4%, and 263.8% at volumetric ratios of 0.4, 0.8, and 1.2, respectively, while peak loads increased by 27.0%, 27.5%, and 31.5%, respectively. Among the three types of fibers used, concrete produced with polypropylene (PP) fibers exhibited the lowest strength results [213].

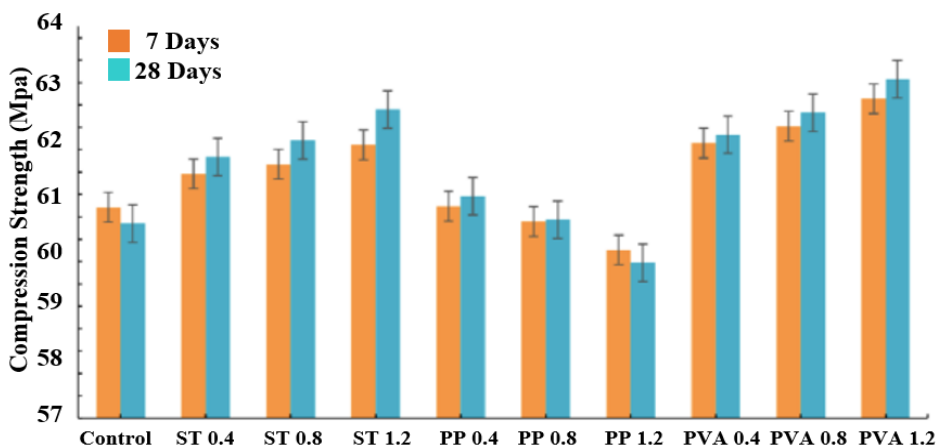


Figure 3.5. Compressive strength of geopolymer mortars according to fibre types and ratios [213]

Gao et al. (2017) investigated the effect of fiber length on the compressive strength and flexural behavior of fiber-reinforced geopolymer composites. They utilized Class F fly ash and blast furnace slag as aluminosilicate, a mixture of sodium silicate and sodium hydroxide as the activator, sand with a maximum particle size of 2 mm as fine aggregate, limestone powder as filler, and 6 and 13 mm steel fibers as reinforcement. Fibers were added to the fresh mix in different combinations of fully long, fully short, and various ratios of the two, with volumetric additions of 0.25, 0.50, 0.75, and 1.00. Curing was conducted at 20°C and 95% relative humidity for 7 and 28 days. The produced 40x40x160 mm mortar specimens underwent a three-point bending test with a loading speed of 0.1 mm/minute. The researchers found that using only short fibers resulted in up to a 31.8% increase in flexural strength, although there was no change in the fracture mode of the specimen, indicating a brittle failure similar to the fiber-free mortar. In contrast, when long fibers were used, flexural strengths increased by up to 58.5%. Moreover, at fiber contents of 0.50, 0.75, and 1.00, a transition to a ductile failure mode was observed [214].

Chi et al. (2018) examined the flexural behavior of geopolymer composites produced using chopped basalt fibers and carbon woven fabric. Plates of composites were prepared using the hand lay-up method with different numbers of layers and various fiber combinations. The composite formulation included metakaolin, sodium silicate, and silica sand with a maximum particle size of 1.25 mm as the resin. The researchers highlighted significant effects of both continuous and discontinuous fibers on flexural strength and toughness. An image of the carbon woven fabric used in the study is shared in Figure 3.6 [215].

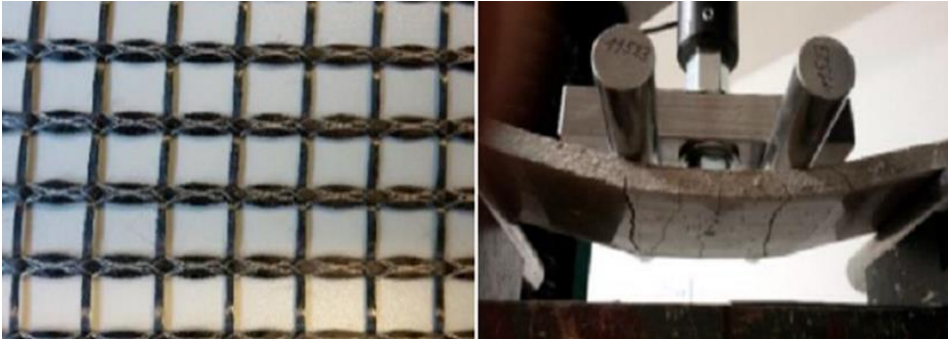


Figure 3.6. The application of carbon fiber weaving and flexural strength testing [215]

Yan et al. (2016) investigated the mechanical properties and microstructures of carbon felt-reinforced geopolymer composites produced using metakaolin obtained by burning kaolin at 800°C for 2 hours and potassium silicate solution as the resin. Carbon felt layers were used in different numbers, with total fiber volumes of 0%, 2.5%, 4.0%, 5.0%, and 5.5%. The geopolymer slurry was impregnated with carbon felt fibers, and the resulting layers were pressed, followed by vacuum drying to prevent void formation. Subsequently, the samples were cured at 60°C for 7 days and subjected to testing. The researchers reported that the addition of carbon felt fibers increased both peak load and corresponding displacements in the load-displacement curve. Depending on the fiber content, they observed increases in flexural strengths ranging from 37.5% to 221.8% and fracture toughness increases in the range of 67.7% to 309.7% [216].

Al-Mashhadani (2021) examined the flexural and compressive strengths of geopolymer SIFCONs produced with different fibers. The study utilized blast furnace slag containing 40.6% SiO₂, 12.8% Al₂O₃, 1.1% Fe₂O₃, and 35.6% CaO, silica fume with 91.6% SiO₂, a 12 M sodium hydroxide solution as the activator, sodium silicate solution with 27.0% SiO₂ and 8.2% Na₂O, river sand with a maximum particle size of 2 mm as aggregate, and steel fibers with hooked ends (30 mm length), crimped steel fibers (36 mm length), and plastic, nylon, and synthetic twisted fibers (40-45 mm length) as reinforcement. Each type of fiber was used to prepare an individual SIFCON. The study selected an activator solution/binder ratio of 0.5, filler/binder ratio of 2.25, and a silica fume/slag ratio of 1. After placing the fibers in the molds, the slurry was poured into the mold, vibrated for compaction, and the specimens were cured for 28 days under ambient conditions. For compressive strength testing, 50 mm cube specimens were used, while 40x40x160 mm prismatic specimens were used for flexural strength. According to the 28-day compressive and flexural strength test results, the

compressive strengths ranged approximately from 42 to 65 MPa, and flexural strengths ranged approximately from 32 to 45 MPa. The study noted that the SIFCON with hooked-end steel fibers exhibited the highest compressive and flexural strengths, attributing this to fiber-matrix adhesion and the mechanical properties of the fibers [217].

Lin et al. (2010) conducted an in-situ structural study to examine crack development in samples. Short carbon fiber-reinforced geopolymer composites have been utilized as refractory material for metal casting at temperatures exceeding 1400°C [16, 218]. The ability of these composites to withstand high temperatures and thermal shock has allowed their use for several casting cycles. Microcracks were observed on the surface layer, but they did not significantly affect the overall performance of the material [17].

Geopolymer composites containing alumina fibers were studied by Zhao et al. (2007) and Foerster et al. (1995). The studies confirm that alumina fibers significantly enhance the flexural strength of a geopolymer matrix. Particularly, the ratio of alumina fibers in the content has a substantial effect on the maximum flexural strength (almost over two-fold) when compared to the maximum flexural strength of the composite matrix. The reported fracture behaviors exhibit consistency, slight deviation from linearity, and a decrease in stress-strain curve around the maximum stress. Heating to 800°C had little effect on the strength of unreinforced geopolymer, but composites with short alumina fibers showed about a 50% decrease in strength after this heat treatment. The combination of short alumina fibers and steel mesh increased the strength and ductility of these composites, preserving these properties even after exposure to high temperatures [17, 219].

Geopolymer composites containing wollastonite (CaSiO_3) microfibers [221], organic PVA fibers [222, 223, 224], and polypropylene (PP) fibers [225, 226] have also been investigated. In each case, the addition of a small amount of fibers increased the strength and toughness of the composite. Lowry and Kriven (2010) reported a maximum three-point flexural strength of approximately 18 MPa for composites containing 2.5% by weight of 2 mm long PP fibers, representing a tenfold increase in strength compared to the unreinforced metakaolin-based matrix [17, 226].

3.4. Production of Geopolymer Additive Brake Friction Materials

The approaches derived or developed for the production of alternative friction linings particularly rely on the use of an inorganic 'alkali-activated' material binder, which exploits the hydraulic activity of certain components capable of

complete hardening when exposed to an alkaline environment (such as high pH values) [54].

Geopolymer materials play a varied role in brake pads, with their function changing based on usage. Some studies refer to them as filling materials within composite structures, while others utilize them as binders [54, 89].

To produce brake pads from geopolymer or composites, the raw materials of geopolymer need to be adjusted initially. For the production of the geopolymer matrix, chemicals such as non-ionized water (distilled), KOH (potassium hydroxide), NaOH (sodium hydroxide), and Na_2SiO_3 (sodium silicate) are used to prepare the activating solution. Alkali activators can sometimes be used in combinations. For example, Na_2SiO_3 is used in combination with NaOH to enhance the geopolymerization process [227]. As for aluminum-silicate sources, suitable materials with content structures such as kaolin, metakaolin, fly ash, ground blast furnace slag, silica fume, and red mud are preferred. Some of these aluminum-silicates are natural products, while others are presented as products resulting from industrial waste or recycling [154, 227]. The alkali activator solution is then mixed with the prepared aluminum-silicate to ensure a homogeneous mixture. A paste-like product is obtained from this mixture, which is allowed to harden in ambient air for a specific period. Subsequently, the paste placed in molds is cured for a designated time in an oven at a specified temperature [227].

Up to this point, the manufacturing processes are generally identical to the overall geopolymerization process and can be considered the first part of production. The second part of the manufacturing process involves producing geopolymer-reinforced brake pads. In this process, the contribution of the geopolymer produced in the first part is ground into a powder form in a ball mill and added to the other components forming the composite for brake pads. This ensures a homogeneous mixture. The subsequent steps rely on production practices specific to brake pad manufacturing, such as pressing and curing [1].

References

1. Embong, Z., Shahudin, S., Hassan, S., Yusof, M.S., Mahzan, S., Shamsuddin, S., Othman, N.K., Mohd Salleh, M.A.A., 2021. A study of geo-polymer as alternative material in automotive brake pad. *AIP Conference Proceedings* 2339, 020130 (2021); <https://doi.org/10.1063/5.0044196>.
2. Arman, M., Singhal, S., Chopra, P., Sarkar, M., 2018. A review on material and wear analysis of automotive Brake Pad. *Materials Today: Proceedings* 5 (2018) 28305–28312
3. Ikpambese, K.K., Gundu, D.T., Tuleun, L.T., 2014. Evaluation of palm kernel fibers (PKFs) for production of asbestos-free automotive brake pads. *Journal of King Saud University - Engineering Sciences*, Volume 28, Issue 1, 2016, Pages 110-118.
4. Grigoratos, T., Martini, G., 2015. Brake wear particle emissions: a review. *Environ Sci Pollut Res* 22, 2491–2504 DOI 10.1007/s11356-014-3696-8.
5. Muzathik, A. M., Mohd Nizam, Y. B., Ahmad, M. F., Wan Nik, W. B. 2013. The effect of boron on the performance of automotive brake. *World Journal of Engineering* 10(6) (2013) 523-528.
6. Akıncıoğlu, G., Öktem, H., Uygur, I., Akıncıoğlu, S., 2018. Determination of Friction-Wear Performance and Properties of Eco-Friendly Brake Pads Reinforced with Hazelnut Shell and Boron Dusts. *Arabian Journal for Science and Engineering*, 43, 4727-4737.
7. Kosbe, P., Patil, P., Muthukumar, M., Gurunathan, R., 2020. Effect of hexagonal boron nitride (h-BN) inclusion on thermal characteristics of disc brake friction composites. *Diamond & Related Materials* (2020), <https://doi.org/10.1016/j.diamond.2020.107895>
8. Idris, U.D., Aigbodion, V.S., Abubakar, I.J., Nwoye, C.I., 2013. Ecofriendly asbestos free brake-pad: using banana peels. *J. King Saud Univ.-Eng. Sci.*, 1-8.
9. Lee, P.W., Filip, P., 2013. Friction and wear of Cu-free and Sb-free environmental friendly automotive brake materials. *Wear*, 302, 1404-1413.
10. Gurunath, P.V., Bijwe, J., 2007. Friction and wear studies on brake-pad materials based on newly developed resin. *Wear*, 263, 1212-1219.
11. Kukutschova, J., Filip, P., 2018. Review of Brake Wear Emissions: A Review of Brake Emission Measurement Studies: Identification of Gaps and Future Needs. *Non-Exhaust Emissions*, 123-146, <https://doi.org/10.1016/B978-0-12-811770-5.00006-6>.

12. Bijwe, J., Nidhi, Majumdar, N., Satapathy, B.K., 2005. Influence of modified phenolic resins on the fade and recovery behavior of friction materials. *Wear* 259, pp 1068-1078 doi:10.1016/j.wear.2005.01.011.
13. Tang, J., Liu, X., Chang, X., Ji, X., Zhou, W., 2022. Elastic geopolymer based on nanotechnology: Synthesis, characterization, properties, and applications. *Ceramics International*,48,5965–5971.
14. Pacheco-Torgal, F., Dollahnejad, Z. Ab., Amoes, A.F.C., Jamshidi, M., Ding, Y., 2012. Durability of alkali-activated binders: a clear advantage over Portland cement or an unproven issue? *Construct. Build. Mater.* 30, 400–405.
15. Davidovits, J., 1991. Geopolymer: ultra-high temperature tooling material for the manufacture of advanced Composites. *Society for the Advancement of Material and Process Engineering Journal*, 2, 1939-1949.
16. Comrie, D.C., Kriven, W.M., 2003. Composite cold ceramic geopolymer in a refractory application. *Ceramic Transactions*,153, 211– 225.
17. Mackenzie, K.J.D., Welter, M., 2014. Geopolymer (aluminosilicate) composites: synthesis, properties and applications. *Advances in Ceramic Matrix Composites*, Pages 445-470. <https://doi.org/10.1533/9780857098825.3.445>.
18. Davidovits, J., 2008a. *Geopolymer, Chemistry and Applications*. Institut Geopolymere, Saint-Quentin, France-4th editions.
19. Cioffi, R., Maffucci, L., Santoro, L., 2003. Optimisation of geopolymer synthesis by calcinations and polycondensation of a kaolinitic residue. *Resources Conservation and Recycling*, 40, 27-8 .
20. Komnitsas, K., Zaharaki, D., 2007. Geopolymerisation: a review and prospects for minerals industry. *Minerals Engineering*, 20, 1261-1277.
21. Lyon, R.E., Balaguru, P.N., Sorathia, U., Foden, A., Sorathia, U., Davidovits, Davidovics, M., 1997. Fire resistant aluminosilicate Composites. *Fire and Materials*, 21, 67 – 73.
22. He, P., Jia, D., Lin, M., Wang, M., Zhou, Y., 2010. Effects of high temperature heat treatment on the mechanical properties of unidirectional carbon fiber reinforced geopolymer Composites. *Ceramics International*, 36, 1447-1453.
23. Bakharev, T., 2006. Thermal behaviour of Geopolymers prepared using class F fly ash and elevated temperature curing. *Cement and Concrete Research*, 36:6, 1134-1147.
24. Rashad, A.M., Zeedan, S.R., 2011. The effect of activator concentration on the residual strength of alkali-activated fly ash pastes subjected to thermal load. *Construction and Building Materials*, 25(7):3098–107.

25. Zhang, Z., Provis, J.L., Reid, A., Wang, H., 2014. Geopolymer foam concrete: An emerging material for sustainable construction. *Construction and Building Materials*, 56, 113–127.
26. Rickard, W.D.A., Williams, R., Temuujin, J., Van Riessen, A., 2011. Assessing the suitability of three Australian fly ashes as an aluminosilicate source for geopolymers in high temperature applications. *Mater Sci Eng A*, 528(9):3390–7.
27. Bai, T., Song, Z., Wang, H., Wu, Y., Huang W., 2019. Performance evaluation of metakaolin geopolymer modified by different solid wastes. *Journal of Cleaner Production*, 226, 114-121.
28. Österle, W., Prietzel, C., Kloß, H., Dmitriev, A.I., 2010. On the role of copper in brake friction materials. *Tribology International*, 43, 2317–2326.
29. Straffelini, G., Ciudin, R., Ciotti, A., Gialanella, S., 2015. Present knowledge and perspectives on the role of copper in brake materials and related environmental issues: a critical assessment. *Environmental Pollution*; Volume 207, Pages 211-219.
30. Bhatt, B., Kalel, N., Ameta, S., Mittal S., Bijwe, J., 2021. Fe–Al alloy for eco-friendly copper-free brake-pads. *Tribology International* 163, 107156.
31. Ayogwu, D.O., Sintali, I.S., Bawa, M.A., 2020. A Review on Brake Pad Materials and Methods of Production. *Composite Materials*. 4(1): 8-14, doi: 10.11648/j.cm.20200401.12
32. Blau, P. J., 2001. Compositions, Functions and Testing of Friction Brake Materials and Their Additives. U.S. Department of Energy, Energy Efficiency and Renewable Energy, Transportation Technologies. Tennessee: Oak Ridge National Laboratory, pp. 78-80.
33. Daei, A.R., Davoudzadeh, N., Filip, P., 2016. Optimization of Brake Friction Materials Using Mathematical Methods and Testing. *SAE International Journal of Materials and Manufacturing*, Vol. 9, No. 1, pp. 118-122.
34. Dahlke, B., Larbig, H., Scherzer, H., Poltrock, R., 1998. Natural fiber reinforced foams based on renewable resources for automotive interior applications. *Journal of Cellular Plastics* 34, 361–379.
35. Roubicek, V., Raclavska, H., Juchelkova, D., Filip, P., 2008. Wear and environmental aspects of composite materials for automotive braking industry. *Wear*, 265, 167–175.
36. Neis, P.D., Ferreira, N.F., Da Silva, F.P., 2014. Comparison between methods for measuring wear in brake friction materials. *Wear*, 319, 191–199. <https://doi.org/10.1016/j.wear.2014.08.004>.

37. Rashid, B., Leman, Z., Jawaid, M., Ishak, M.R., Al-Oqla, F.M., 2017. Eco-Friendly Composites for Brake Pads From Agro Waste: A Review. *Encyclopedia of Materials: Composites*. Volume 3, Pages 209-228.
38. Drava, G., Leardi, R., Portesani, A., Sales, E., 1996. Application of Chemometrics to the Production of Friction Materials: Analysis of Previous Data and Search of New Formulations. *Chemometrics and Intelligent Laboratory System*, 32:2, 245-255.
39. Cox, Roy L., 2012. Engineered tribological composites: the art of friction material development. SAE International, USA, ISBN 978-0-7680-3485-1; SAE Order Number R-401; DOI 10.4271/R-401.
40. Selvam, P.T., Pugazhenthir., Dhanasekaran, C., Chandrasekaran, M., Sivaganesan, S., 2021. Experimental investigation on the frictional wear behaviour of TiAlN coated brake pads. *Materials Today: Proceedings*, Volume 37, Part 2, Pages 2419-2426.
41. Cai, P., Wang, Y., Wang, T., Wang, Q., 2015. Effect of resins on thermal, mechanical and tribological properties of friction materials. *Tribology International*, 87, 1–10.
42. Barros, L.Y., Neis, P.D., Ferreira, N.F., Pavlak, R.P., Masotti, D., Matozo, L.T., Sukumaran, J., De Baets, P., Andó, M., 2016. Morphological analysis of pad-disc system during braking operations. *Wear*; 352–353, p112-121. <https://doi.org/10.1016/j.wear.2016.02.005>.
43. Kumar, S., Ghosh, S.K., 2019. Particle emission of organic brake pad material: a review. *J Automobile Eng*; 158, p1–10. [https://doi.org/DOI: 10.1177/0954407019879839](https://doi.org/DOI:10.1177/0954407019879839).
44. Aranganathan, N., Mahale, V., Bijwe, J., 2016. Effects of aramid fiber concentration on the friction and wear characteristics of non-asbestos organic friction composites using standardized braking tests. *Wear*; 354–355, 69–77. <https://doi.org/10.1016/j.wear.2016.03.002>.
45. Eriksson, M., Lord, J., Jacobson, S., 2001. Wear and contact conditions of brake pads: dynamical in situ studies of pads on glass. *Wear*; 249, p272–278. [https://doi.org/10.1016/S0043-1648\(01\)00573-7](https://doi.org/10.1016/S0043-1648(01)00573-7).
46. Kumar, S., Ghosh, S.K., 2020. Porosity and tribological performance analysis on new developed metal matrix composite for brake pad materials. *Journal of Manufacturing Processes*, 59, 186–204.
47. Hee, K.W., Filip, S.P., 2005. Performance of Ceramic-Enhanced Phenolic Matrix Brake Lining Materials for Automotive Brake Linings. *Wear*, Vol. 259, pp. 1088-1096.

48. Eriksson, M., Jacobson, S., 2000. Tribological surfaces of organic brake pads. *Tribology International*, 33: 817-827, doi:10.1016/S0301-679X(00)00127-4.
49. Blau, P.J., 2001. Compositions, Functions, and Testing of Friction Brake Materials and Their Additives. Oak Ridge National Laboratory Report ORNL/TM 2001/64. Oak Ridge, TN, 24 pp.
50. Chan, D., Stachowiak, G., 2004. Review of automotive brake friction materials. *Proceedings of the Institution of Mechanical Engineers, Part D: Journal of Automobile Engineering*, 218: 953-964, doi:10.1243/0954407041856773.
51. Aras, S., Tarakçioğlu, N., 2021. Optimization and assessment of brake pad production parameters and organic Juniperus drupacea cone powder additive ratio using the Taguchi method. *Journal of Composite Materials*, 1-15. doi: 10.1177/0021998321997532.
52. Cho, M.H., Ju, J., Kim, S.J., Jang, H., 2006. Tribological properties of solid lubricants (graphite, Sb_2S_3 , MoS_2) for automotive brake friction materials. *Wear*, 260: 855-860, 2006, doi:10.1016/j.wear.2005.04.003.
53. Saffar, A., Shojaei, A., 2012. Effect of rubber component on the performance of brake friction materials. *Wear*, 274-275: 286-297, 2012, doi:10.1016/j.wear.2011.09.012.
54. Sanguineti, A., Tosi, F., Bonfanti, A., 2016. Alkali-Activated Inorganic Based Brake Pads: Realization and Performances of Alternative Friction Materials for a Concrete Industrial Application. SAE Technical Paper, doi:10.4271/2016-01-1913.
55. Qi, S., Fu, Z., Yun, R., Jiang, S., Zheng, X., Lu, Y., Matejka, V., Kukutschova, J., Peknikova, V., Prikasky, M., 2014. Effects of walnut shells on friction and wear performance of eco-friendly brake friction composites. *Proceedings of the Institution of Mechanical Engineers Part J; Journal of Engineering Tribology*, 228(5), 511-520. SAGE.
56. Aranganathan, N., Bijwe, J., 2016. Development of copper-free eco-friendly brake friction material using novel ingredients. *Wear*, 352-353, 79-91.
57. Xiao, X., Yin, Y., Bao, J., Lijian, L., Feng, X., 2016. Review on friction and wear of brake materials. *Advances in Mechanical Engineering*, vol. 8(5), 1-10.
58. Jadhav, S.P., Sawant, S.H., 2019. A review paper: Development of novel friction material for vehicle brake pad application to minimize environmental and health issues. *Materials Today: Proceedings*, vol 19, Part 2, 209-212.

59. Torgal, F.P., Gomes, J.C., Jalali, S., 2008. Alkaliactivated binders: A review. Part 2. About materials and binders manufacture. *Construction and Building Materials*, 22:1315-1322, doi:10.1016/j.conbuildmat.2007.03.019.015.
60. Rashad, A.M., 2013. Alkali-activated metakaolin: A short guide for civil engineering-An overview. *Construction and Building Materials*, 41: 761-765, <https://doi.org/10.1016/j.conbuildmat.2012.12.030>.
61. Provis, J.L., Palomo, A., Shi, C., 2015. Advances in understanding alkali-activated materials. *Cement and Concrete Research*, 78:110-125, <http://dx.doi.org/10.1016/j.cemconres.2015.04.013>.
62. Lee, P.W, Lee, L., Filip, P., 2013. Friction Performance of Eco-Friendly Cu-Free Brake Materials with Geopolymer Matrixes. *SAE Int. J. Passeng. Cars - Mech. Syst.*, 6(3): doi:10.4271/2013-01-2026.
63. Mahale, V., Bijwe, J., Sinha, S., 2019. A step towards replacing copper in brake-pads by using stainless steel swarf. *Wear*: 424–425,133–142.
64. Singh, T., Patnaik, A., Chauhan, R., 2016. Optimized selection of cement kiln dust filled brake pad formulation for best tribo-performance properties using grey relation analysis approach. *Materials & Design*, Vol. 89, 1335-1342.
65. Jeganmohan, S.R., Christy, T.V., Solomon, D.G., Sugoza, B., 2020. Influence of calcium sulfate whiskers on the tribological characteristics of automotive brake friction materials. *Engineering Science and Technology, an International Journal*, Vol 23: 2, 445-451.
66. Yashwhanth, S., Mithun Mohan, M., Anandhan, R., Selvaraj, S.K., 2021. Present knowledge and perspective on the role of natural fibers in the brake pad material. *Materials Today: Proceedings*: 46,7329–7337.
67. Saha, D., Sharma, D., Satapathy, B.K., 2023. Challenges pertaining to particulate matter emission of toxic formulations and prospects on using green ingredients for sustainable eco-friendly automotive brake composites. *Sustainable Materials and Technologies*:37, e00680.
68. Sekiguchi, I., Kubota, K., Oyanagi, Y., Kosaka, M., Sone, Y., 1992. Tribological properties of COPNA resin. *Wear*, Vol. 158:1-2, 171-183.
69. Zhang, G., Ke, Y., Qin, M., Shen, H., Xu, J., 2015. Preparations and tribological properties of COPNA copolymer materials. *Procedia Engineering*: 102, 615-624.
70. Yusubov, F., 2021. Tribiological behavior of modified phenolic resin composites for braking applications. *Industrial Lubrication and Tribology*, Vol. 73 No. 5, pp. 775-782. <https://doi.org/10.1108/ILT-05-2020-0175>.

71. Liu, Y., Schaefer, Y.A., 2006. The sliding friction of thermoplastic polymer composites tested at low speeds. *Wear*: 261,568–577
72. Park, J., , Song, W., Seo, H., Lee, J.J., Kwon, S.U., Jang, H., 2022. Effect of thermoplastic polymer in brake pads on particulate matter emission: A case study with polyethylene. *Tribology International*: 173,107629.
73. Lawal, S.S., Ademoh, N.A . Bala, K.C. Abdulrahman, A.S., 2019. A Review of the Compositions, Processing, Materials and Properties of Brake Pad Production. *Journal of Physics: Conference Series*:1378, 032103.
74. Pulikkalparambil, H., Babu, A., Thilak, A., Vighnesh, N.P., Rangappa, S.M., Siengchin, S., 2023. A review on sliding wear properties of sustainable biocomposites: Classifications, fabrication and discussions. *Heliyon*: 9, e14381. <https://doi.org/10.1016/j.heliyon.2023.e14381>
75. Ra, I., 2015. Effect of date palm seeds on the tribological behaviour of polyester composites under different testing conditions. *J. Mater. Sci. Eng.:* 4, <https://doi.org/10.4172/2169-0022.1000206>.
76. Cho, K.H., Jang, H., Hong, Y.S., Kim, S.J., Basch, R.H., Fash, J.W., 2008. The size effect of zircon particles on the friction characteristics of brake lining materials. *Wear*: 264, 291-297.
77. El-Tayeb, N.S.M., Liew, K.W., 2009. On the dry and wet sliding performance of potentially new frictional brake pad materials for automotive industry. *Wear*: 266, 275-287. doi:10.1016/j.wear.2008.07.003.
78. Akıncıoğlu, G., Akıncıoğlu, S., Uygur, I., Öktem, H., 2018. Bor oksit tozunun fren balatalarının tribolojik özelliklerine etkisi. *Sakarya Üniversitesi Fen Bilimleri Enstitüsü Dergisi*: 22 (2), 755-760. Doi:10.16984/aufenbilder.352785.
79. Ikpambese, K.K., Gundu, D.T., Tuleu, L.T., 2014. Evaluation of palm kernel fibers (PKFs) for production of asbestos-free automotive brake pads. *Journal of King Saud University-Engineering Sciences*, 28:1, 110-118. <http://dx.doi.org/10.1016/j.jksues.2014.02.001>.
80. Sugözü, B., Buldum, B.B., Sugözü, İ., 2018. Üleksit ve boraks içeren fren sürtünme malzemelerinin tribolojik özellikleri. *BORON*, 3: 2, 125-131. DOI: 10.30728/boron.365196.
81. Sagirolu, S., Akdogan, K., 2023. The effect of the addition of blast furnace slag on the wear behavior of heavy transport polymer-based brake pads. *Tribology International*, 189, 108845. <https://doi.org/10.1016/j.triboint.2023.108845>.
82. Öztürk, B., Öztürk, S., Adigüzel, A.A., 2013. Effect of Type and Relative Amount of Solid Lubricants and Abrasives on the Tribological Properties

of Brake Friction Materials, *Tribology Transactions*, 56:3, 428-441, DOI: 10.1080/10402004.2012.758333.

83. Yanar, H., Purcek, G., Demirtas, M., Ayar, H.H., 2022. Effect of Hexagonal Boron Nitride (h-BN) Addition on Friction Behavior of Low-Steel Composite Brake Pad Material for Railway Applications, *Tribology International*, 165. 107274. doi: <https://doi.org/10.1016/j.triboint.2021.107274>.
84. Wan Nik, W.B., Ayob, A.F., Syahrullail, S., Masjuki, H.H., Ahmad, M.F., 2012. The Effect of Boron Friction Modifier on The Performance of Brake Pads. *International Journal of Mechanical and Materials Engineering (IJMME)*, Vol. 7: 1, 31–35.
85. Rajkumar, K., Gnanavelbabu, A., Venkatesan, M.S., Rajagopalan, K., 2018. Cooperating Function of Graphite in Reducing Frictional Wear of Aluminium Boron Carbide composite Materials Today: *Proceedings*, 5: 14 (2), 27801-27809. <https://doi.org/10.1016/j.matpr.2018.10.016>.
86. Sankar, M., Gnanavelbabu, A., Rajkumar, K., 2014. Effect of reinforcement particles on the abrasive assisted electrochemical machining of Aluminium-Boron carbide-Graphite composite. *Procedia Engineering*, 97, 381-389. <https://doi.org/10.1016/j.proeng.2014.12.262>.
87. Akıncıoğlu, G., Akıncıoğlu, S., Uygur, I., Öktem, H., 2019. Alternatif katkı maddesi olarak kullanılan bor oksitinin fren balatasının sürtünme davranışına etkisinin incelenmesi. *BORON*, 4:1, 1-6. Doi: 10.30728/boron.405788.
88. Muzathik, A.M., Mohd Nizam, Y.B., Ahmad, M.F., Wan Nik, W.B., 2013. The effect of boron on the performance of automotive brake. *World Journal of Engineering*, 10:6. 523-528. Doi: 10.1260/1708-5284.10.6.523.
89. Savetlana, S., Zulhanif, Z., Supriadi, H., Ramadhan, I., Beliantara, T., 2022. The Effect of Barite Addition and Graphite Particle Size on The Specific Abrasion of Fly-Ash/Phenolic Composite for Brake Lining Application. *Journal of Engineering and Scientific Research*, Vol. 4:1, 8-13. <https://doi.org/10.23960/jesr.v4i1.102>.
90. Yang, Y., Liang, L.X., Wu, H., Liu, B.W., Qu, H., Fang, Q.H., 2020. Effect of zinc powder content on tribological behaviors of brake friction materials. *Trans. Nonferrous Met. Soc. China*, 30. 3078-3092. Doi:10.1016/S1003-6326(20)65444-9.
91. Zhang, P., Zhang, L., Wu, P., Cao, J., Shijia, C., Wei, D., Qu, X., 2020. Effect of carbon fiber on the braking performance of copper-based brake pad under continuous high-energy braking conditions. *Wear*, 458-459, 203408. <https://doi.org/10.1016/j.wear.2020.203408>.

92. Faga, M.G., Casamassa, E., Iodice, V., Sin, A., Gautier, G., 2019. Morphological and structural features affecting the friction properties of carbon materials for brake pads. *Tribology International*, 140, 105889. <https://doi.org/10.1016/j.triboint.2019.105889>.
93. Singh, T., Gehlen, G.S., Ferreira, N.F., Barros, L.Y., Lasch, G., Poletto, J.C., Ali, S., Neis, P.D., 2023. Automotive brake friction composite materials using natural *Grewia Optiva* fibers. *Journal of Materials Research and Technology*, 26, 6966-6983. <https://doi.org/10.1016/j.jmrt.2023.09.072>.
94. Pathmanaban, P., Aalam, A.M., Selvaganesh, A., Iamrishi, S.Sr, 2019. Testing of Coconut Shell Reinforced Brake Pads. *International Journal of Scientific Research and Engineering Development*. 2:5, 853-859.
95. Dan-Asabe, B., Madakson, P.B., Manji, J., 2012. Material Selection and Production of a Cold-Worked Composite Brake Pad. *World J. Eng. Pure Appl. Sci.*, 2:3, 92-97.
96. Elakhame, Z.U., Olotu, O.O., Abiodun, Y.O., Akubueze, E.U., Akinsanya, O.O., Kaffo, P.O., Oladele, O.E., 2017. Production of Asbestos Free Brake Pad Using Periwinkle Shell as Filler Material, *International Journal of Scientific & Engineering Research*, 8:6, 1728-1735.
97. Bhakuni, H., Muley, A.V., Ruchika, 2023. Fabrication, testing & analysis of particulate ceramic matrix Composite for automotive brake pad application. *Materials Today: Proceedings*, <https://doi.org/10.1016/j.matpr.2023.01.413>.
98. Başar, G., Buldum, B.B., Sugözü, İ., 2018. Kolemanit ve Boraks Takviyeli Fren Balatalarının Sürtünme Performansı. *El-Cezerî Journal of Science and Engineering*, 5:2, 635 -644.
99. Bashir, M., Saleem, S.S., Bashir, O., 2015. Friction and Wear Behavior of Disc Brake Pad Material Using Banana Peel Powder. *International Journal of Research in Engineering and Technology*. 4:2, 650-659.
100. Kalel, N., Bhatt, B., Darpe, A., Bijwe, A., 2021. Copper-free brake-pads: A break-through by selection of the right kind of stainless steel particles. *Wear*. 464-465. doi: <https://doi.org/10.1016/j.wear.2020.203537>.
101. Bijwe, J., Kumar, M., 2007. Optimization of steel wool contents in non-asbestos organic (NAO) friction composites for best combination of thermal conductivity and tribo-performance. *Wear*. 263:7-12, 1243-1248. Doi: <https://doi.org/10.1016/j.wear.2007.01.125>.
102. Vijay, R., Janesh, M.J., Saibalaji, M.A., Thiyagarajan, V., 2013. Optimization of Tribological Properties of Nonasbestos Brake Pad

Material by Using Steel Wool. *Advances in Tribology*. Doi: <http://dx.doi.org/10.1155/2013/165859>.

103. Pattanaik, A., Satpathy, M.P., Mishra, S.C., 2016. Dry sliding wear behavior of epoxy fly ash composite with Taguchi optimization. *Engineering Science and Technology, an International Journal*, 19:2, 710-716. <http://dx.doi.org/10.1016/j.jestch.2015.11.010>.
104. Yilmaz, A.C., 2022. Effects of fly ash introduction on friction and wear characteristics of brake pads. *International Journal of Automotive Engineering and Technologies*. 11:3, 96-103. <https://doi.org/10.18245/ijaet.1108124>.
105. Singaravelu, D.L., Vijay, R., Filip, P., 2019. Influence of various cashew friction dusts on the fade and recovery characteristics of non-asbestos copper free brake friction composites. *Wear*, 426–427. 1129-1141. <https://doi.org/10.1016/j.wear.2018.12.036>.
106. Kukutschova, J., Moravec, P., Tomasek, V., Matejka, V., Smolik, J., Schwarz, J., Seidlerova, J., Safarova, K., Filip, P., 2011. On airborne nano/micro-sized wear particles released from low-metallic automotive brakes, *Environmental Pollution*. 159, 998-1006.
107. Akmal, J., Zulhendri, H., Su'udi, A., Hidayatullah, T., 2018. Study of Carbon Fiber And Sulfur Reinforced Geopolymers Composite for Train's Brake Blocks. *Prosiding SNTTM XVII, Oktober 2018*, hal. 149-154. ISSN 2623-0313.
108. Saindane, U.V., Soni, S., Menghani, J.V., 2021. Studies on mechanical properties of brake friction materials derived from carbon fibres reinforced polymer composite. *Materials Today: Proceedings*. 47:17, 5760-5765.
109. Chandradass, J., Sethupathi, P.B., Surabi, M.A., 2021. Fabrication and characterization of asbestos free epoxy based brake pads using carbon fiber as reinforcement. *Materials Today: Proceedings*, 45, 7222-7227. <https://doi.org/10.1016/j.matpr.2021.02.530>.
110. Öztürk, B., Arslan, F., Öztürk, S., 2007. Hot wear properties of ceramic and basalt fiber reinforced hybrid friction materials. *Tribology International*, 40:1, 37-48. <https://doi.org/10.1016/j.triboint.2006.01.027>.
111. <https://www.marathonbrake.com/tech-support/raw-materials/full-story/>, (10.01.2024).
112. <https://auto.howstuffworks.com/auto-parts/brakes/brake-parts/brake-pads.htm>, (10.01.2024).
113. <https://www.hella.com/partnerworld/uk/Product-range/XBrake-system/Brake-pads-2968/>, (10.01.2024).

114. <https://www.patsgarage.com/brake-pad-replacement-san-francisco/>, (10.01.2024).
115. <https://www.powertech-auto.com/how-brake-pad-manufactured-process/>, (10.01.2024).
116. <https://www.fluidtherm.com/pages/brochure-downloads-a/furnaces-for-pm-industry.pdf>, (10.01.2024).
117. <https://www.gasbarre.com/products/furnace/furnace-by-product/cvcq-lam-vacuum-sintering-furnaces/>, (11.01.2024).
118. <https://www.pm-review.com/introduction-to-powder-metallurgy/sintering-in-the-powder-metallurgy-process/>, (11.01.2024).
119. <https://www.nationalbronze.com/News/understanding-the-powdered-metal-process-spot-light-on-compacting/>, (11.01.2024).
120. Gutiérrez, J.G., Stringari, G.B., Emri, I., 2012. Powder Injection Molding of Metal and Ceramic Parts. Some Critical Issues for Injection Molding. DOI: 10.5772/38070.
121. <https://www.armstrongcn.com/hot-press-machine-product/>, (12.01.2024).
122. Guo, H., Bayer, T.J.M., Guo, J., Baker, A., Randal, C.A., 2017. Current progress and perspectives of applying cold sintering process to ZrO₂-based ceramics. *Scripta Materialia*, 136, 141-148. Doi: <https://doi.org/10.1016/j.scriptamat.2017.02.004>.
123. <https://www.labor.com.tr/urun/retsch-emax-yuksek-enerjili-bilyali-ogutucu-besleme-malzemesi-orta-sert-sert-kirilgan-lifli-kuru-veya-islak-malzeme-giris-buyuklugu-lt-5-mm-cikis-bu-yuklugu-lt-80-nm-ogutucu-istasyon-sayisi-2>, (12.01.2024).
124. <https://dal.aku.edu.tr/2016/11/13/karistirici-bilyali-spex-degirmen/>, (12.01.2024).
125. https://www.analitika.com.tr/uploaded/urunler/19/1563894672_up-lab-atritors.pdf, (12.01.2024).
126. <https://www.toztek.com/3d-mikser.html>, (12.01.2024).
127. <https://acesprocess.com/blog/karistirma-makineleri/>, (12.01.2024).
128. Davidovits, J., 1989. Geopolymer and geopolymeric materials. *Journal of Thermal Analysis*, 35, 429-441. Doi: 10.1007/BF01904446
129. Davidovits, J., 2017. Review. Geopolymers: Ceramic-Like Inorganic Polymers. *J. Ceram. Sci. Technol.*, 8:3, 335-350. Doi: 10.4416/JCST2017-00038.
130. Jiang, C., Wang, A., Bao, X., Ni, T., Ling, J., 2020. A review on geopolymer in potential coating application: Materials, preparation and basic properties. *Journal of Building Engineering*, 32, 101734. <https://doi.org/10.1016/j.jobbe.2020.101734>.

131. Kozhukhova, N., Kozhukhova, M., Zhernovskaya, I., Promakhov, V., 2020. The Correlation of Temperature-Mineral Phase Transformation as a Controlling Factor of Thermal and Mechanical Performance of Fly Ash-Based Alkali-Activated Binders. *Materials*, 13, 5181. doi:10.3390/ma13225181.
132. Provis, J.L., van Deventer, J.S.J., 2009. *Geopolymers: Structure, processing, properties and industrial applications*. Woodhead Publishing Limited and CRC Press LLC: Woodhead Publishing Limited, Abington Hall, Granta Park, Great Abington, Cambridge CB21 6AH, UK. Published in North America by CRC Press LLC, 6000 Broken Sound Parkway, NW, Suite 300, Boca Raton, FL 33487, USA.
133. Shi, C., Roy, D., Krivenko, P., 2014, Alkali-activated cements and concretes, CRC Press, 392. <https://doi.org/10.1201/9781482266900>.
134. Ng, C., Alengaram, U.J., Wong, L.S., Mo, K.H., Jumaat, M.Z., Ramesh, S., 2018. A review on microstructural study and compressive strength of geopolymer mortar, paste and concrete. *Construction and Building Materials*, 186, 550–576.
135. Duxson, P., Provis, J.L., Lukey, G.C., van Deventer, J.S., 2007. The role of inorganic polymer technology in the development of ‘green concrete’. *Cement and Concrete Research*, 37:12,1590-1597.
136. Chindapasirt, P., Sata, V., Pangdaeng, S., Sinsiri, T., 2007. Workability and strength of coarse high calcium fly ash geopolymer. *Cement and Concrete Composites*, 29,224-229.
137. Rangan, B.V., Hardjito, D., Wallah, S.E., Sumajouw, M.J., 2005. Studies on fly ash-based geopolymer concrete. *Proceedings of world congress geopolymer*, France.
138. Sing, N.S., Middendorf, B., 2020. Geopolymers as an alternative to Portland cement: An overview. *Construction and Building Materials*. 237. <https://doi.org/10.1016/j.conbuildmat.2019.117455>.
139. Wallah, S.E., Rangan, B.V., 2006. Low –calcium fly ash based geopolymer concrete: long-term properties. Research Report GC2, Faculty of Engineering, Curtin University of Technology, Perth, Australia, 1-97, 2006.
140. Reddy, M.S., Dinakar, P., Rao, B.H., 2016. A review of the influence of source material’s oxide composition on the compressive strength of geopolymer concrete. *Microporous and Mesoporous Materials*, 234, 12-23.
141. Zhuang, X.Y., Chen, L., Komarneni, S., Zhou, C.H., Tong, D.S., Yang, H.M., Yu, W.H., Wang, H., 2016. Fly ash-based geopolymer: clean

- production, properties and applications. *Journal of Cleaner Production*, 125, 253-267. <https://doi.org/10.1016/j.jclepro.2016.03.019>.
142. Davidovits, J., 2002. 30 years of successes and failures in geopolymer applications, market trends and potential breakthroughs. In: *Geopolymer 2002 Conference*. Saint-Quentin (France), Melbourne (Australia): Geopolymer Institute.
143. Dimas, D., Giannopoulou, I., Panyas, D., 2009. Polymerization in sodium silicate solutions: a fundamental process in geopolymerization technology. *J Mater Sci.*, 44:14, 3719-3730. <https://doi.org/10.1007/s10853-009-3497-5>.
144. Hounsi, A.D., Lecomte-Nana, G., Djeteli, G., Blanchart, P., Alowanou, D., Kpelou, P., Napo, K., Tchangbedji, G., Praisler M., 2014. How does Na, K alkali metal concentration change the early age structural characteristic of kaolin-based geopolymers. *Ceramics International*, 40, 8953-8962.
145. Zheng, C., Wang, J., Liu, H., GangaRao, H., Liang, R., 2022. Characteristics and microstructures of the GFRP waste powder/GGBS-based geopolymer paste and concrete. *Reviews on Advanced Materials Science*. 61, 117-137. <https://doi.org/10.1515/rams-2022-0005>.
146. <https://www.nbmw.com/product-technology/construction-chemicals/waterproofing/concrete-admixtures/geopolymer-concrete-the-eco-friendly-alternate-to-concrete.html>. (14. 12. 2023).
147. Cong, P., Cheng, Y., 2021. Advances in geopolymer materials: A comprehensive review. *Journal of Traffic and Transportation Engineering (English Edition)*, 8: 3, 283-314. <https://doi.org/10.1016/j.jtte.2021.03.004>.
148. Jwaida, Z., Dulaimi, A., Mashaan, N., Mydin, M.A.O, 2023. Geopolymers: The Green Alternative to Traditional Materials for Engineering Applications. *Infrastructures*, 8, 98. <https://doi.org/10.3390/infrastructures8060098>.
149. Alakara, E.H., Nacar, S., Sevim, O., Korkmaz, S., Demir, I., 2022. Determination of compressive strength of perlite-containing slag-based geopolymers and its prediction using artificial neural network and regression-based methods, *Construction and Building Materials*. 359,129518, <https://doi.org/10.1016/j.conbuildmat.2022.129518>.
150. Elgarahy, A.M., Maged, A., Eloffy, M.G., Zahran, M., Kharbish, S., Elwakeel, K.Z., Bhatnagar, A., 2023. Geopolymers as sustainable eco-friendly materials: Classification, synthesis routes, and applications in wastewater treatment. *Separation and Purification Technology*. 324, 124631, <https://doi.org/10.1016/j.seppur.2023.124631>.

151. Temuujin, J., Williams, R.P., van Riessen, A., 2009, Effect of mechanical activation of fly ash on the properties of geopolymer cured at ambient temperature. *Journal of Materials Processing Technology*, 209, 5276-5280. <https://doi.org/10.1016/j.jmatprotec.2009.03.016>.
152. Singh, N.B., 2018. Fly ash-based geopolymer binder: a future construction material. *Minerals*, 8:7 299. <https://doi.org/10.3390/min8070299>.
153. De Weerd, K., 2011. *Geopolymers - State of the art*, Oslo : SINTEF Building and Infrastructure. ISSN 1891-1978.
154. Amran, Y. M., Alyousef, R., Alabduljabbar, H., El-Zeadani, M., 2020. Clean production and properties of geopolymer concrete; A review. *Journal of Cleaner Production*, Cilt 251. <https://doi.org/10.1016/j.jclepro.2019.119679>.
155. Palomo, A., Grutzeck, M.W., Blanco, M.T., 1999. Alkali-Activated Fly Ashes: A Cement for the Future. *Cement and Concrete Research*. 29, 1323-1329. [https://doi.org/10.1016/S0008-8846\(98\)00243-9](https://doi.org/10.1016/S0008-8846(98)00243-9).
156. Salahuddin, M.B.M., Norkhairunnisa, M., Mustapha, F., 2015. A review on thermophysical evaluation of alkali-activated Geopolymers. *Ceramics International*, 41, 4273-4281. <http://dx.doi.org/10.1016/j.ceramint.2014.11.119>.
157. Davidovits, J., 2011. *Geopolymer chemistry and applications*. (3rd ed.). France: Geopolymer Institute.
158. Yip, C.K., Lukey, G.C., Provis, J.L., Van Deventer, J.S.J., 2008. Effect of calcium silicate sources on geopolymerisation. *Cement and Concrete Research*, 38, 554-564. Doi: 10.1016/j.cemconres.2007.11.001.
159. Wang, K., Shah, S. P., Mishulovich, A., 2004. Effects of curing temperature and NaOH addition on hydration and strength development of clinker-free CKD-fly ash binders. *Cement and Concrete Research*, 34:2, 299-309. Doi:10.1016/j.cemconres.2003.08.003.
160. Hager, I., Sitarz, M., Mróz, K., 2021. Fly-ash based geopolymer mortar for high-temperature application–Effect of slag addition. *Journal of Cleaner Production*, 316, 128168. <https://doi.org/10.1016/j.jclepro.2021.128168>.
161. Shvarzman, A., Kovler, K., Grader, G.S., Shter, G.E., 2003, The effect of dehydroxy-lation/amorphization degree on pozzolanic activity of kaolinite. *Cement and Concrete Research*, 33:3, 405-416. [https://doi.org/10.1016/S0008-8846\(02\)00975-4](https://doi.org/10.1016/S0008-8846(02)00975-4).
162. Mobili, A., Belli, A., Giosuè, C., Bellezze, T. ve Tittarelli, F., 2016. Metakaolin and fly ash alkali-activated mortars compared with cementitious mortars at the same strength class. *Cement and Concrete Research*, 88, 198-210. <https://doi.org/10.1016/j.cemconres.2016.07.004>.

163. Duan, P., Yan, C., Luo, W., 2016. A novel waterproof, fast setting and high early strength repair material derived from metakaolin Geopolymer. *Construction and Building Materials*, 124, 69-73. <https://doi.org/10.1016/j.conbuildmat.2016.07.058>.
164. Sun, Z., Vollpracht, A., 2018. Isothermal calorimetry and in-situ XRD study of the NaOH activated fly ash, metakaolin and slag. *Cement and Concrete Research*, 103, 110-122. <https://doi.org/10.1016/j.cemconres.2017.10.004>.
165. Davidovits, J., 2008b. *Geopolymer chemistry and applications*, 3rd edition, Institut Geopolymere, St. Quinten, 398-406.
166. Davidovits, J., 1991. Geopolymers: inorganic polymeric new materials. *Journal of Thermal Analysis and Calorimetry*, 37:8, 1633-1656. <https://doi.org/10.1007/bf01912193>.
167. Davidovits, J., 2008c. *Geopolymer Chemistry and Applications*. Second Edition, Institut Géopolymère, France, 584 p.
168. Pelisser, F., Guerrino, E.L., Menger, M., Michel, M.D., Labrincha, J.A., 2013. Micromechanical characterization of metakaolin-based Geopolymers. *Construction and Building Materials*, 49, 547-553. <https://doi.org/10.1016/j.conbuildmat.2013.08.081>.
169. Rovnaník, P., Al, S.O., 2010. Effect of curing temperature on the development of hard structure of metakaolin-based geopolymer. *Construction and Building Materials*, 24:7, 1176-1183. <https://doi.org/10.1016/j.conbuildmat.2009.12.023>.
170. Lahoti, M., Narang, P., Tan, K.H., Yang, E., 2017. Mix design factors and strength prediction of metakaolin-based geopolymer. *Ceramics International*, 43:14, 11433-11441. <https://doi.org/10.1016/j.ceramint.2017.06.006>.
171. Zhang, H. Y., Kodur, V., Qi, S.L., Cao, L., Wu., B., 2014. Development of metakaolin-fly ash based geopolymers for fire resistance applications. *Construction and Building Materials*, 55, 38-45. <https://doi.org/10.1016/j.conbuildmat.2014.01.040>.
172. Srividya, T., Kannan Rajkumar, P.R., Sivasakthi, M., Sujitha, A., Jeyalakshmi, R., 2022. A state-of-the-art on development of geopolymer concrete and its field applications. *Case Studies in Construction Materials*, 16, e00812. <https://doi.org/10.1016/j.cscm.2021.e00812>.
173. Davidovits, J., 1999. *Chemistry of Geopolymeric Systems*, Terminology, International Conference, France. ISBN:2902933150, 2902933142.
174. Lyu, Y., Leonardi, M., Wahlström, J., Gialanella, S., Olofsson, U., 2020. Friction, wear and airborne particle emission from Cu-free brake materials.

175. Mathur, R., Thiyagarajan, P., Dhami, T., 2004. Controlling the hardness and tribological behaviour of non-asbestos brake lining materials for automobiles. *Journal of Carbon Science*, 5:1, 6-11. 1976-4251(pISSN).
176. Surojo, E., Malau, V., Ilman, M., 2014. Effects of phenolic resin and fly ash on coefficient of friction of brake shoe composite. *Journal of Engineering & Applied Sciences*, 9:11, 2234-2240.
177. Kim, Y.C., Cho, M.H., Kim, S.J., Jang, H., 2008. The effect of phenolic resin, potassium titanate, and CNSL on the tribological properties of brake friction materials. *Wear*, 264: (3-4), 204-210. <https://doi.org/10.1016/j.wear.2007.03.004>.
178. Bijwe, J., 2007. NBR-modified resin in fade and recovery module in non-asbestos organic (NAO) friction materials. *Tribology Letters*, 27, 189-196. Doi: 10.1007/s11249-007-9225-x.
179. Soboyejo, W., 2003. *Mechanical Properties of Engineered Materials*, Marcel Dekker, Inc. 270 Madison Avenue, New York, NY 10016, ISBN: 0-8247-8900-8.
180. Raja, V.K.B., Raj, S.K., Sairam, M.D., Kasyap, A.V.R.S., Kumar, V.G., Padmapriya, R., Baalamurugan, J., Sonawane, P.D., 2021. Geopolymer green technology. *Materials Today: Proceedings*, 46:2, 1003-1007. <https://doi.org/10.1016/j.matpr.2021.01.138>.
181. Nikoloutsopoulos, N., Sotiropoulou, A., Kakali, G., Tsivilis, S., 2021. Physical and Mechanical Properties of Fly Ash Based Geopolymer Concrete Compared to Conventional Concrete. *Buildings*, 11:5, 178. <https://doi.org/10.3390/buildings11050178>.
182. van Jaarsveld, J.G.S. , van Deventer , J.S.J., Lukey , G.C., 2003. The characterization of source materials in fly ash- based Geopolymer. *Materials Letters*, 57.7, 1272-1280. [https://doi.org/10.1016/S0167-577X\(02\)00971-0](https://doi.org/10.1016/S0167-577X(02)00971-0).
183. Ferone, C., Colangelo, F., Roviello, G., Asprone, D., Menna, C., Balsamo, A., Prota, A., Cioffi, R., Manfredi, G., 2013. Application-Oriented Chemical Optimization of a Metakaolin Based Geopolymer. *Materials*, 6, 1920-1939. <https://doi.org/10.3390/ma6051920>.
184. Castillo, H., Collado, H., Droguett, T., Sánchez, S., Vesely, M., Garrido, P., Palma, S., 2021. Factors Affecting the Compressive Strength of Geopolymers: A Review. *Minerals*, 11, 1317. <https://doi.org/10.3390/min11121317>.

185. Rodríguez, E., Mejía de Gutiérrez, R., Bernal, S., Gordillo, M., 2009. Effect of the $\text{SiO}_2/\text{Al}_2\text{O}_3$ and $\text{Na}_2\text{O}/\text{SiO}_2$ ratios on the properties of geopolymers based on MK. *Revista Facultad de Ingeniería Universidad de Antioquia*, 49, 30-41.
186. Yunsheng, Z., Wei, S., Zongjin, L., 2010. Composition design and microstructural characterization of calcined kaolin-based geopolymer cement. *Applied Clay Science*, 47: (3-4), 271-275. <https://doi.org/10.1016/j.clay.2009.11.002>.
187. Chen, L., Wang, Z., Wang, Y., Feng, J., 2016. Preparation and Properties of Alkali Activated Metakaolin-Based Geopolymer. *Materials*, 9, 767. <https://doi.org/10.3390/ma9090767>.
188. Rovank, P., 2010. Effect of curing temperature on the development of the hard structure of metakaolin-based geopolymer. *Construction and Building Materials*, 24:7, 1176-1183, <https://doi.org/10.1016/j.conbuildmat.2009.12.023>.
189. Zhang, H., Li, L., Sarker, P.K., Long, T., Shi, X., Wang, Q., Cai, G., 2019. Investigating Various Factors Affecting the Long-Term Compressive Strength of Heat-Cured Fly Ash Geopolymer Concrete and the Use of Orthogonal Experimental Design Method. *International Journal of Concrete Structures and Materials*, 13, 63. <https://doi.org/10.1186/s40069-019-0375-7>.
190. Duxson, P., Provis, J., Lukey, G.C., Mallicoat, S.W., Kriven, W.M., van Deventer, J.S., 2005. Understanding the relationship between geopolymer composition, microstructure and mechanical properties. *Colloids and Surfaces A: Physicochem. Eng. Aspects*, 269: (1-3), 47-58. <https://doi.org/10.1016/j.colsurfa.2005.06.060>.
191. Duxson, P., Mallicoat, S., Lukey, G., Kriven, W., van Deventer, J., 2007. The effect of alkali and Si/Al ratio on the development of mechanical properties of metakaolin-based geopolymers. *Colloids and Surfaces A: Physicochem. Eng. Aspects*, 292:1, 8-20. <https://doi.org/10.1016/j.colsurfa.2006.05.044>.
192. Zhao, S., Xia, M., Yu, L., Huang, X., Jiao, B., Li, D., 2021. Optimization for the preparation of composite geopolymer using response surface methodology and its application in lead-zinc tailings solidification. *Construction and Building Materials*, 266, 120969. <https://doi.org/10.1016/j.conbuildmat.2020.120969>.
193. Singh, S., Aswath, M., Ranganath, R., 2018. Effect of mechanical activation of red mud on the strength of geopolymer binder. *Construction and*

Building Materials, 177, 91-101. <https://doi.org/10.1016/j.conbuildmat.2018.05.096>.

194. Kuranchie, F.A., Shukla, S.K., Habibi, D., 2014. Utilisation of iron ore mine tailings for the production of geopolymer bricks. *International Journal of Mining, Reclamation and Environment*, 30:2, 92-114. <https://doi.org/10.1080/17480930.2014.993834>.
195. Lemougna, P.N., Nzeukou, A., Aziwo, B., Tchamba, A.B., Wang, K., Melo, U.C., Cui, X., 2020. Effect of slag on the improvement of setting time and compressive strength of low reactive volcanic ash geopolymers synthesized at room temperature, *Materials Chemistry and Physics*, 239, 122077, <https://doi.org/10.1016/j.matchemphys.2019.122077>.
196. Kolousek, D., Brus, J., Urbanova, M., Andertova, J., Hulinsky, V., Vorel, J., 2007. Preparation, structure and hydrothermal stability of alternative (sodium silicate- free) geopolymers. *Journal of Materials Science*, 42, 9267-9275. <https://doi.org/10.1007/s10853-007-1910-5>.
197. Brew, D.R.M., MacKenzie, K.J.D., 2007. Geopolymer synthesis using silica fume and sodium aluminate, *Journal of Materials Science*, 42, 3990-3993. Doi: 10.1007/s10853-006-0376-1.
198. Brooks, R., Bahadory, M., Tovia, F, Rostami, H., 2010. Properties of alkali-activated fly ash: high performance to lightweight, *International Journal of Sustainable Engineering*, 3:3, 211-218. <https://doi.org/10.1080/19397038.2010.487162>.
199. Ravikumar, D., Peethamparan, S., Neithalath, N., 2010. Structure and strength of NaOH activated concretes containing fly ash or GGBFS as the sole binder. *Cement and Concrete Composites*, 32, 399-410. Doi: 10.1016/j.cemconcomp.2010.03.007.
200. Barbosa, V.F.F., MacKenzie, K.J.D., 2003. Thermal behavior of inorganic geopolymers and composites derived from sodium polysialate. *Materials Research Bulletin*, 38, 319-331. [https://doi.org/10.1016/S0025-5408\(02\)01022-X](https://doi.org/10.1016/S0025-5408(02)01022-X).
201. Barbosa, V.F.F., MacKenzie, K.J.D., 2003. Synthesis and thermal behavior of potassium sialate geopolymers. *Materials Letters*, 57: (9-10), 1477-1482. Doi:10.1016/S0167-577X(02)01009-1.
202. Bell, J.L., Driemeyer, P.E., Kriven, W.M., 2009. Formation of ceramics from metakaolin- based geopolymers. Part I Cs- based Geopolymers. *Journal of the American Ceramic Society*, 92, 1-8. Doi: 10.1111/j.1551-2916.2008.02790.x.

203. Provis, J.L., van Deventer, J.S.J., 2009. *Geopolymers: Structure, Processing, Properties and Industrial Applications*, Woodhead Publishing, Oxford. ISBN: 978-1-84569-449-4.
204. Cheng, T.W., Chiu, J.P., 2003. Fire- resistant geopolymer produced by granulated blast furnace slag. *Minerals Engineering*, 16, 205-210. doi:10.1016/S0892-6875(03)00008-6.
205. Lyon, R.E. , Sorathia, U. , Balaguru, P. , Foden, A. , Davidovits, J., Davidovics, M., 1997. Fire- resistant aluminosilicate Composites. *Fire and Materials*, 21:2, 67-73. [https://doi.org/10.1002/\(SICI\)1099-1018\(199703\)21:2<67::AID-FAM596>3.0.CO;2-N](https://doi.org/10.1002/(SICI)1099-1018(199703)21:2<67::AID-FAM596>3.0.CO;2-N).
206. Soleimani, M.A., Naghizadeh, R., Mirhabibi, A.R., Golestanifard, F., 2013. The Influence of Phosphorus Slag Addition on Microstructure And Mechanical Properties of Metakaolin-Based Geopolymer Pastes. *Journal Ceramics-Silikáty*, 57:1, 33-38. ISSN: 0862-5468
207. Bernal, S.A., Provis, J.L., Rose, V., Gutierrez, R.M., 2011. Evolution of binder structure in sodium silicate –activated slag-metakaolin blends. *Cement and Concrete Composites*, 33:1, 46-54. Doi: 10.1016/j.cemconcomp.2010.09.004.
208. Midhun, M.S., Rao, T.D.G., Srikrishna, T.C., 2018. Mechanical and fracture properties of glass fiber reinforced geopolymer concrete. *Advances in Concrete Construction*, 6:1, 29-45. <https://doi.org/10.12989/acc.2018.6.1.029>.
209. Chu, S.H., Ye, H., Huang, L., Li, L.G., 2021. Carbon fiber reinforced geopolymer (FRG) mix design based on liquid film thickness, *Construction and Building Materials*, 269, 121278. <https://doi.org/10.1016/j.conbuildmat.2020.121278>.
210. Guo, X., Xiong, G., 2021, Resistance of fiber-reinforced fly ash-steel slag based geopolymer mortar to sulfate attack and drying-wetting cycles, *Construction and Building Materials*, 269:121326. <https://doi.org/10.1016/j.conbuildmat.2020.121326>.
211. He, P., Jia, D., Lin, M., Wang, M., Zhou, Y., 2010. Effects of high temperature heat treatment on the mechanical properties of unidirectional carbon fiber reinforced geopolymer Composites. *Ceramics International*, 36:4, 1447-1453. <https://doi.org/10.1016/j.ceramint.2010.02.012>.
212. Behera, P., Baheti, V., Militky, J., Louda, P., 2018. Elevated temperature properties of basalt microfibril filled geopolymer composites. *Construction and Building Materials*, 163, 850-860. <https://doi.org/10.1016/j.conbuildmat.2017.12.152>.

213. Al-Mashhadani, M.M.M., Canpolat, O., Aygörmez, Y., Uysal, M., Erdem, S., 2018, Mechanical and microstructural characterization of fiber reinforced fly ash based geopolymer composites. *Construction and Building Materials*, 167, 505-513. <https://doi.org/10.1016/j.conbuildmat.2018.02.061>.
214. Gao, X., Yu, Q.L., Yu, R., Brouwers, H.J.H., 2017. Evaluation of hybrid steel fiber reinforcement in high performance geopolymer composites, *Materials and Structures*, 5:165,1-14. Doi:10.1617/s11527-017-1030-x.
215. Chi, H.L., Louda, P., Periyasamy, A.P., Bakalova, T. and Kovacic, V., 2018. Flexural behavior of carbon textile-reinforced geopolymer composite thin plate, *Fibers*, 6:4, 87. <https://doi.org/10.3390/fib6040087>.
216. Yan, S., He, P., Jia, D., Yang, Z., Duan, X., Wang, S. and Zhou, Y., 2016. Effect of fiber content on the microstructure and mechanical properties of carbon fiber felt reinforced geopolymer composites, *Ceramics International*, 42:6, 7837-7843. <https://doi.org/10.1016/j.ceramint.2016.01.197>.
217. Al-Mashhadani, M.M.M., 2021. Strength behavior of geopolymer based SIFCON with different fibers, *European Journal of Science and Technology*, Special Issue 28,1342-1347. <https://doi.org/10.31590/ejosat.1015350>.
218. Lin, T., Jia, D., He, P., Wang, M., 2010. In situ crack growth observation and fracture behavior of short carbon fibre reinforced geopolymer matrix composites. *Material Science and Engineering A*, 527, 2404-2407. Doi:10.1016/j.msea.2009.12.004.
219. Zhao, Q., Nair, B., Rahimian, T., Balaguru, P., 2007. Novel geopolymer based composites with enhanced ductility. *Journal of Materials Science*, 42, 3131-3137. Doi:10.1007/s10853-006-0527-4.
220. Förster, S.C., Graule, T., Gauckler, L.J., 1995. Thermal and mechanical properties of alkali- activated alumino- silicate based high performance composites. *Advances in Science and Technology*, 7, 117-124.
221. Silva, F.J., Thaumaturgo, C., 2003. Fibre reinforcement and fracture response in geopolymeric mortars. *Fatigue and Fracture of Engineering Materials and Structures*, 26:2, 167-172. <https://doi.org/10.1046/j.1460-2695.2003.00625.x>.
222. Yunsheng, Z., Sun, W., Li, Z., 2006. Impact behavior and microstructural characteristics of PVA fibre reinforced fly ash geopolymer boards prepared by extrusion technique, *Journal of Materials Science*, 41, 2787-2794. Doi: 10.1007/s10853-006-6293-5.

223. Yunsheng, Z., Sun, W., Li, Z., Zhou, X., Eddie, Chungkong, C., 2008. Impact properties of geopolymer based extrudates incorporated with fly ash and PVA short fiber. *Construction and Building Materials*, 22:3, 370-383. Doi:10.1016/j.conbuildmat.2006.08.006.
224. Sun, P., Wu, H., 2008. Transition from brittle to ductile behaviour of fly ash using PVA fibers, *Cement and Concrete Composites*, 30:1, 29-36. Doi:10.1016/j.cemconcomp.2007.05.008.
225. Zhang, Z., Yao, X., Zhu, H., Hua, S., Chen, Y., 2009. Preparation and mechanical properties of polypropylene fiber reinforced calcined kaolin-fly ash based Geopolymer. *Journal of Central South University of Technology*, 16, 49-52. Doi: 10.1007/s11771-009-0008-4.
226. Lowry, D.R., Kriven, W.M., 2010. Effect of high tensile strength polypropylene chopped fiber reinforcements on the mechanical properties of sodium based Geopolymer Composites. *Ceramic Engineering and Science Proceedings*, 31:10, 47-56. ISSN: 0196-6219. <https://doi.org/10.1002/9780470944103.ch5>.
227. Al Bakri, A.M.M., Kamarudin, H., Bnhussain, M., Liyana, J., Ghazali, C.M.R., 2013. Nano Geopolymer for Sustainable Concrete Using Fly Ash Synthesized by High Energy Ball Milling. *Applied Mechanics and Materials*, 313,169-173. Doi: 10.4028/www.scientific.net/AMM.313-314.169